Spatial and Temporal Variation of Land Surface Temperature in New Guinea and Borneo Island

Munawar

A Thesis Submitted in Fulfillment of the Requirements for the Degree of Doctor of Philosophy in Research Methodology Prince of Songkla University 2022

Thesis Title   Spatial and Temporal Variation of Land Surface Temperature
in New Guinea and Borneo Island

Author   Mr. Munawar

Major Program   Research Methodology

Major Advisor

…………………………………………
(Assist. Prof. Dr. Rhysa McNeil)

Co-Advisor

…………………………………………
(Assoc. Prof. Dr. Rohana Jani)

…………………………………………
(Emeritus Prof. Dr. Don McNeil)

Examining Committee:

……………………………... Chairperson
(Asst. Prof. Dr. Sangdao Wongsai)

……………………………. Committee
(Asst. Prof. Dr. Phattrawan Tongkumchum)

……………………………. Committee
(Asst. Prof. Dr. Mayuening Eso)

……………………………. Committee
(Asst. Prof. Dr. Rhysa McNeil)

……………………………. Committee
(Assoc. Prof. Dr. Rohana Jani)

……………………………. Committee
(Emeritus Prof. Dr. Don McNeil)

       The Graduate School, Prince of Songkla University, has approved this thesis as the fulfilment of the requirements for the Doctor of Philosophy Degree in Research Methodology.
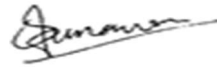

…………………………………….…...
(Prof. Dr. Damrongsak Faroongsarng)
Dean of Graduate School

This is to certify that the work here submitted is the result of the candidate's own investigations. Due acknowledgement has been made of any assistance received.

………………………………Signature

(Asst. Prof. Dr. Rhysa McNeil)

Major Advisor

………….………………….…Signature

(Mr. Munawar)

Candidate

I hereby certify that this work has not been accepted in substance for any other degree,

and is not being currently submitted in candidature for any degree.

………………...………………….…Signature

(Mr. Munawar)

Candidate

Thesis Title   Spatial and Temporal Variation of Land Surface Temperature

in New Guinea and Borneo Island

Author   Mr. Munawar

Major Program   Research Methodology

Academic Year   2021

ABSTRACT

Increased temperature is one of the signals of global warming. Land Surface Temperature (LST) can be used to measure climate change. This study aimed to investigate the pattern and variation of LST on New Guinea and Borneo Island using a cubic spline and a multivariate regression model. The correlation between LST and the normalized difference vegetation index (NDVI) was also examined using Pearson correlation. The LST and NDVI data were obtained from 2000 to 2019 from the National Aeronautics and Space Administration Moderate Resolution Imaging Spectroradiometer database for each sub-region.

New Guinea was divided into two analyses**.** The first analysis consisted of 45 sub-regions (210-pixels distance) while the second analysis consisted of 90 sub-regions (105-pixels) on the island. The overall mean increase of LST per decade for 45 sub-regions was $+0.012^{o}C$ with a 95% confidence interval $(-0.052, 0.077)^{o}C$. The 90 sub-regions had a significant overall mean increase in LST of $+0.086^{o}C$, with 95% confidence interval $(0.028, 0.144)^{o}C$.

The first analysis the result show that there were two super-regions A (north-west) and C (central-south) that had significant mean decrease and increase of LST with $-0.107^{o}C$ and $0.201^{o}C$ respectively. The second analysis had five super-regions with significant mean variation of LST. There were four super-regions with the

mean LST increase in B1 (central-north1), C1 (central-south1), C2 (central-south2) and E2 (south-east2) with 0.008ºC, 0.042ºC, 0.185ºC, 0.217ºC, respectively, and one of super-region of A2 (north-west2) has mean LST decrease by -0.122ºC.

Borneo Island was divided into eight super-regions with a 105-pixel distance between sub-regions resulting in 72 sub-regions covering the entire island. The overall mean increase in LST was +0.203ºC per decade with 95% confidence interval (0.138, 0.267). The changes differed by region; a significant increase was found in Sarawak, North Kalimantan, West Kalimantan, West-central Kalimantan, Central-east Kalimantan region, and a slight decrease was seen in Sabah and Brunei Darussalam (Sabah & Brunei) region. There was a slight increase in East Kalimantan and a stable trend in South Kalimantan.

The correlations between LST and NDVI in Boneo Island were low and varied for each sub-region. Most of the correlations in the sub-regions were positive. Most of the sub-regions showed that the pattern of LST and NDVI were similar at the beginning and the end of the year.

Keywords: LST, NDVI, Cubic spline, Pearson, New Guinea Island, Borneo Island

Acknowledgements

I would like to express my deepest gratitude to Prof. Dr. Don McNeil, Asst. Prof. Dr. Rhysa McNeil, and Assoc. Prof. Dr. Rohana Jani for their countless help, inspiration, and guidance. I also express my gratitude to Asst. Prof. Dr. Phattrawan Tongkumchum, Asst. Prof. Dr. Rattikan Saelim, Asst. Prof. Dr. Sarawut Chesoh, Assoc. Prof. Dr. Apirade Lim, Asst. Prof. Dr. Mayuening Eso, all lecturers and staff at Research Methodology Program, Department of Mathematics and Computer Science, Faculty of Science and Technology, Prince of Songkla University, Thailand, for their support. I appreciate Thailand's Education Hub for ASEAN Countries (TEH AC) scholarship and the Prince of Songkla Graduate School grant.

I would like to extend my gratitude to my lovely wife, son, daughter, late father, mommy, father-in-law, late mother-in-law, uncle, and aunt (for their funding), late sister and brother, sisters and brother, my colleagues at Statistics Department, Mathematics and Sciences Faculty, Syiah Kuala University, Indonesia. All my friends from Indonesia and Thailand, which I cannot enumerate for their kindness.

Munawar

Contents

Contents (cont.)

List of figures

List of figures (cont.)

List of tables

Chapter 1

Introduction

This chapter consists of background and rationale, research objective, literature review, and thesis organization.

1.1 Background and rationale

The earth has been facing climate change problems lately because of the greenhouse effect. Climate change indicators showed a variation in the increase of global carbon dioxide and temperature. The impacts of climate change were water availability (Wang et al., 2007), changes in extremes of temperature and precipitation, decreased seasonal and perennial snow and ice extent (Karl and Trenberth, 2003). Sea-level raised, biodiversity and ecosystem services at risk (Cruz et al., 2007), human health as the effect of increasing the prevalence rate for a particular disease (Checkley et al., 2000), and the spread of infectious bacteria (Pascual et al., 2002).

Global temperature over one century was increased on average $0.6^{\circ}C$ and increased rapidly (Houghton et al., 2001). South-east Asia has become warmer, ranging from $0.09^{\circ}C$ to $0.24^{\circ}C$ per decade between 1973 – 2008 (Chooprateep and McNeil, 2014). Estoque et al. (2017) stated that the temperature of some megacities in Southeast Asia is estimated to be $0.3^{\circ}C$ higher than the temperature of the green area.

South-east Asia also has been affected by the climate change problem. The development will damage the environment and increase people who need food, housing, and industrial support. Forests will be sacrificed for the fulfillment of food or agriculture, housing, and city development. South-east Asia has the tallest tropical

rainforests globally with the most significant timber volumes, involved in the high logging levels in this region (Davis et al., 2001). The development of the timber industry and the expansion of the palm area have resulted in forest damage affecting flora.

New Guinea is the second-largest island in the world after Greenland. It is divided into two territories between Indonesia in the west and Papua New Guinea in the east. The Pacific Ocean surrounds the island on the north and east, Australia in the south, and Sulawesi Island in the west. The study about New Guinea Island Land Surface Temperature (LST) is critical because New Guinea LST variation would influence the LST of the surrounding island. The prediction of New Guinea temperature was increased by about $0.4 - 1.0^{\circ}C$ per decade (International Climate Change Adaptation Initiative (ICCAI), 2007). A report claimed that extreme temperature was one factor in the significant disappearance of appropriate habitations for plant species in Papua and Papua New Guinea (Robiansyah, 2018). Another study found that in the southern Pacific region, including Papua and Papua New Guinea, the annual and seasonal ocean surface and island air temperatures have risen by 0.6 to $1.0^{\circ}C$ since 1910 (Folland et al., 2003).

As part of southeast Asia island, Borneo Island is a centre of biological diversity, with 68% flora and fauna are found (Collins et al., 1991). McAlpine et al. (2018) found that the equatorial island-like Borneo is a deforestation hotspot. Borneo has lost 40–75% of its forests since 1973. According to the island width, there is a strong relationship between forest loss, daily temperature increases, and precipitation reductions. The expansion of agricultural and industrial areas such as oil palm,

pulpwood plantation, and rice projects for transmigration caused forest loss and fragmentation in Borneo Island (Langner et al., 2007).

Borneo has become the main area for oil palm in Malaysia and Indonesia. The total 30% oil palm land in 2003 was in Sabah, accompanied by 12% in Sarawak Malaysia. Kalimantan was not as important as Sumatra in Indonesia but enlarging the open area to oil palm has been remarkable. The 5.25 million hectares of Indonesian land under oil palm in 2003, approximately 19% was in Kalimantan contrasted to 72% in Sumatra (Cooke, 2006), Borneo Island becomes principal island since the Indonesian Government is planning to move the country's capital to the Borneo Island.

Countries in Borneo Island rely heavily on the forest, agricultural, and aquaculture products. The temperature change will affect the amount and the quality of forest products, crop yield, and fishes' catches. Borneo island temperature is very much influenced by the temperature of other parts of Indonesia include Sumatera, Jawa, Sulawesi, Papua Island, and the immediate surroundings of the South China Sea.

Borneo Island (Indonesian called Kalimantan) consists of three countries: Indonesia, Malaysia, and Brunei Darussalam (Cleary and Lian, 1991). Most of the island area belongs to Indonesia, and the rest be in Malaysia and Brunei Darussalam. Compared to Greenland and New Guinea Island, Kalimantan Island is the third largest island in the world (Heritage, 2020). Kalimantan contains savanna, lowlands, and mountains, with a wide variety of plants and animals as a typical habitat in tropical rain forests (Cleary and Lian, 1991). Utmost temperatures will cause the disappearance of appropriate habitations for animals and plants (Hughes, 2017; Kottawa-Arachchi and Wijeratne, 2017). Borneo average surface temperatures were predicted to rise by 3–5°C

per decade (Tangang et al., 2012). Deforested parts of Borneo had higher temperatures than forested areas (McAlpine et al., 2018).

Indonesia is a country with the largest share area in Southeast Asia which faces problems in climate change. Indonesia's significant impact of climate change includes temperature increase, intense rainfall, sea-level rise, and a threat to food security for the people (Measey, 2010). Indonesia has been experiencing warming from 0.2 to 0.3°C every ten years. Every year, some parts of Indonesia face increased precipitation, except for the southern part, where precipitation usually declines by 15%. The seasonality precipitation fluctuation in some parts of Sumatra and Borneo islands will be at a 10 to 30% wetter level by the 2080s during December-February. Jakarta will be at a 5-15% drier level during June-August. Thirty-day delay in the annual monsoon, at 10% increase in rainfall later in the crop year (April-June), and up to 75% decrease in rainfall later in the dry season (July–September) (Case et al., 2007).

The LST can impart comprehensive into climatological activities, land surface energy association, and water security at global scales (Li et al., 2012; Wongsai et al., 2017), together with climate change results. The climate variations can critically influence human health, the environment, and economic and social progress (Marjuki et al., 2016; Mboera et al., 2011; Mishra et al., 2010). Climate variation has a significant relation with human being disorder vulnerability (Wu et al., 2016). It is manifested in the deceleration of the long period decline in the occurrence of undernutrition, which is connected to extreme climatic events (Wheeler and Braun, 2013). LST is generally utilized to estimate increasing temperatures.

The LST mean continued to rise globally (Mildrexler et al., 2018). In equatorial areas, there have been vast changes in the proportion of rising mean surface

temperatures. The change turns on many factors for instance elevation, normalized difference vegetation index (NDVI), and land cover (LC) (Alavipanah et al., 2015; Sun et al., 2012). The substantial change in Land Elevation (LE) significantly impacts the LST (Gao et al., 2008).

Wan et al. (2004) assessed and validated the quality of the MODIS global LST so that it can be used for better temporal, spatial, and angular coverage of clear-sky observations. Considering temperature escalates formed on enormous-scale satellite imagery data is crucial and primary for future condition integrity (Weigand et al., 2019). Various studies have explored surface temperature trends and patterns applying numerous statistical methods like cubic splines, considerably operated for smoothing data (Wongsai et al., 2017) and linear regression model (McNeil and Chirtkiatsakul, 2016).

This study focused to investigate the pattern and change of day LST on New Guinea Island and Borneo Island applying NASA MODIS data from 2000 to 2019. And to find the correlation between LST change and NDVI on Borneo Island.

1.2. Research objective

The research objectives of this study are:

1. to investigate the seasonal pattern and trend of LST change in the New Guinea Island and Borneo Island

2. to examine the correlation between LST and NDVI in Borneo Island

1.3 Literature review

Some studies have examined the LST seasonal pattern, trend, and variation on New Guinea and Borneo Island with various statistical methods and different sources of data.

Temperature variation on New Guinea Island

The studies on New Guinea Island temperature have been done on a small part of the island, like along the Huon peninsula and Milne Bay province, with the ten- and 40-years data, respectively (Aharon and Chappell, 1986; Davies and Brown, 1997). Aharon and Chappell (1986) used the ice volume to predict the sea surface temperature, and Davies and Brown (1997) used the cut point of the sea surface temperature to predict the corral bleach. Both types of research recorded a different variation of sea surface temperature, and the sea surface temperature influenced the land surface temperature (Yan et al., 2020).

Bourke (2010) observed that most Papua New Guinea latitude ranges 1 - 9ºsouth with the seasonal temperature change in $1 – 2$ºC. Karnieli et al. (2010) found a negative correlation between LST and NDVI using 21 years of data from Advanced Very High-Resolution Radiometer (AVHRR). Another study on the Lae district of Morobe province in Papua New Guinea was calculated the LST from LANDSAT satellite data using a linear model (Samanta, 2009).

The Land Use/Land Cover (LU/LC) changed the earth surface and atmosphere affected human life (Turner et al., 1995). The global LU/LC has an impact in fulfilling the human needs with the expansion of farm, plantation, and urban areas in line with the loss of biodiversity (Foley et al., 2005).

Temperature variation on Borneo Island

A study data in Sarawak of northern Borneo Island was downloaded from National Oceanic and Atmospheric Administration 14 AVHRR. The data used during June – July 1996 to estimate the LST by using atmospheric effect and surface emissivity and found that the difference between LST and satellite temperature is 7°C (Batatia and Bessaih, 1997). How et al. (2009) found that the LST increased +7.5°C on Cameron Highlands, Pahang state, Malaysia, during 2009-2019 due to the change in LU/LC.

Another study, Kemarau and Eboy (2020), found that positive correlation between LST and Natural Difference Built-up Index (NDBI) due to LU/LC change on Kinabalu city for 1991, 2011, and 2018. Hidayati et al. (2020) were used K-means and Fuzzy C-means methods to cluster the climate change variables temperature, precipitation, relative humidity, and wind speed and correlate with the fire forest. The two methods were resulting two negative correlations.

Cubic spline modelling on temperature variation

Cubic spline model not only used to examine the satellite data but widely used in many aspects such as the relationship between temperature and mortality in London (Armstrong, 2006), modelling climate change-driven treeline shifts (Dullinger et al., 2004), biodiesel production modelling (Gülüm et al., 2009), temperature data analysis for supersonic flight test (Sahoo and Peetala, 2010), Transmission covid-19 (Wang et al., 2020). Wongsai et al. (2017) used the cubic spline with MODIS data to investigate the trend of LST with the change of LU/LC in Phuket, Thailand.

Normalized difference vegetation index

Feng et al. (2019) found that, in the spatial pattern of LST research, the candidate spatial factors include: land coverage indices, for example, the NDBI and the

NDVI, and the normalized difference water index (NDWI), proximity factors of a kind that the distances to the city centre, town centres, and major roads, and the LST location.

Yue et al. (2007) stated that LST, NDVI, and Shannon Diversity Index (SHDI) showed a positive correlation between LST and SHDI and a negative correlation between NDVI and SHDI. LST is affected by the land surface characteristics such as vegetation cover, LU/LC, and surface imperviousness. Incessant urbanization often increases in the urban area and has caused significant land surface changes (Khandelwal et al., 2018).

There are three classifications of NDVI based on the LU/LC. The classification and the NDVI value are -1 to 0.199, considered non-vegetation consists of barren areas, build-up area, road network. The value from 0.2 to 0.5 showed as low vegetation comprises shrub and grassland, and the high vegetation value started from 0.501 to 1.0 as a temperate and tropical urban forest (Hashim et al., 2019).

NDVI could explain the LE and LU/LC. The different types of LE have different vegetation types (Mokarram and Sathyamoorthy, 2015). The LC/LU change can be detected by the NDVI category (Aburas et al., 2015). This research has examined the correlation between the LST using only one variable, such as NDVI without LE and LC/LU, to avoid the correlation between NDVI and LE, LC/LU.

Spatial correlation

The climate science researcher faces autocorrelation and spatial problems. The data potentially relate to the other data in terms of time lag, and the climate data between the two areas will affect each other. Those problems will affect inference analysis such as LST (Kestens et al., 2011). A study shows a relationship between space and time in climate research data (Storch and Zwiers, 1999). It is valuable because it can reconstruct

space and time problems in the atmosphere and oceans with fewer observations (Dunstone, 2014). For statistical inference to have a robust result, the process of inferring from a limited sample with a hypothetic statement, the correlation needed independent data (Storch, 1999).

1.4 Organization of thesis

This thesis is organized into five chapters. The first chapter introduces background and rationale, research objective, literature review. Chapter 2 describes all the methodologies used, including the study area, data source, study diagram, and statistical methods. Chapter 3 narrates the LST variation in New Guinea Island. Chapter 4 reports LST and NDVI variation in Borneo Island, and Chapter 5 concludes the discussion and suggestions for further research.

Chapter 2

Methodology

This chapter comprises the study area, data source and data management, variable definitions, statistical method, and study diagram. This chapter also explains the division of the study area, how to download the data, and the flow of study.

2.1 Study area

There are two study areas, one in New Guinea Island and one in Borneo Island.

New Guinea Island

New Guinea Island is located at -11° to 0° south latitude and 130° to 152° east longitude. There are two analyses on New Guinea Island. In the first analysis, the island was divided into five super-regions, with each super region coded from A to E and each consisting of nine sub-regions. We defined the super-regions and sub-regions by optimizing the land than the water surface to avoid missing values. The sub-regions were placed around parallels of 210-pixels of sample line widths (approximately 190 km) apart in tile or image coordinate (210-pixels).

New Guinea Island was divided into Indonesia and Papua New Guinea territory. The sub-region was covered New Guinea Island (Figure 2.1). The super-region A represents the North-West, and super-region B on the Central-North Papua Indonesia. The super-region C reveal on the Central South of the island between Indonesia and Papua New Guinea. The super-region D locates in the North-East, and the super-region E finds in the South-East of Papua New Guinea.
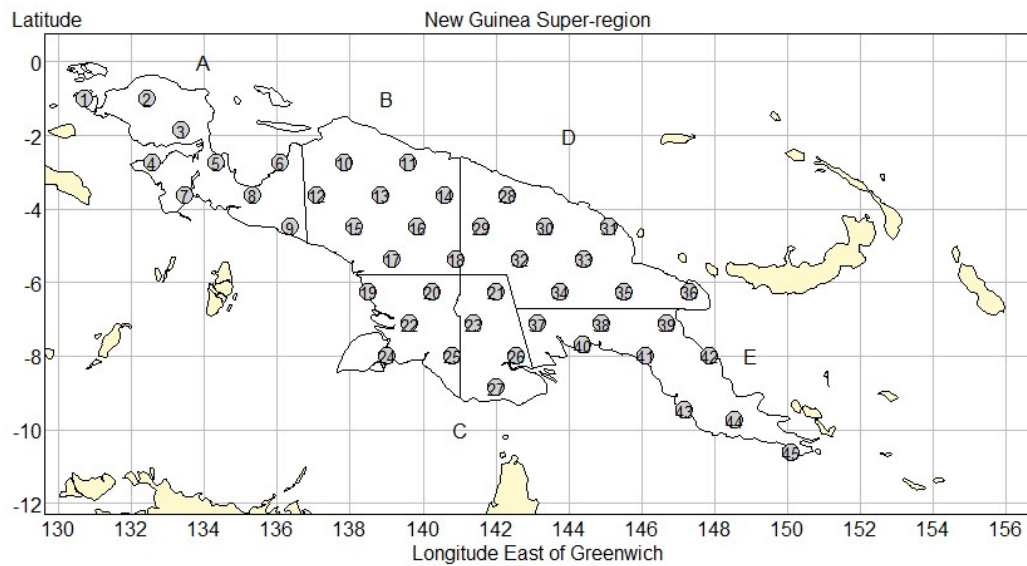
Figure 2.1 First analysis area on New Guinea Island

The second analysis divided the New Guinea Island into ten super-regions, consisting of nine sub-regions (Figure 2.2). The distance between sub-regions was 105-pixels of sample and line widths (95 km) aside in tile coordinates (105-pixels). The sub-regions were distributed with an equal distance covering the New Guinea mainland resulting in 90 sub-regions. The sub-regions of the first analysis were marked in a light grey shade.
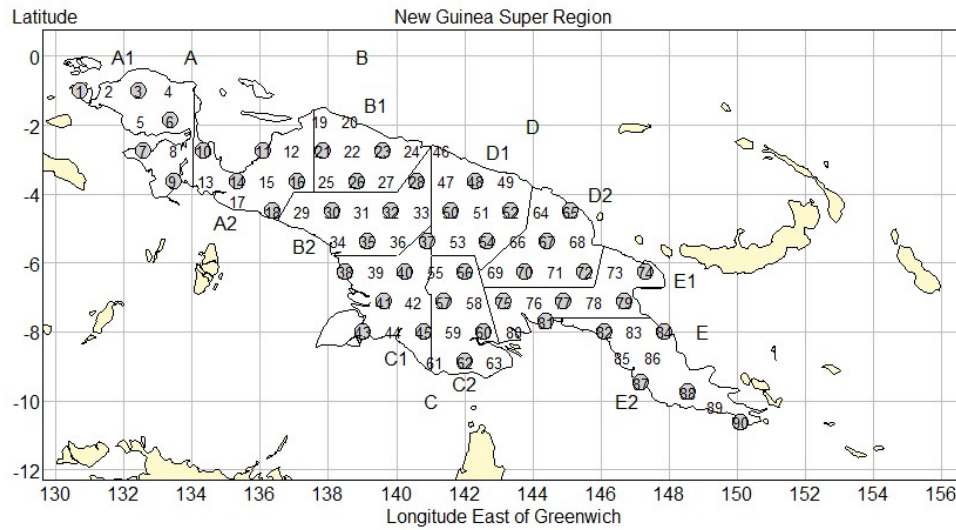
Figure 2.2 Second analysis area on New Guinea Island

Borneo Island

Borneo Island is found at 109° to 119° east longitude and -4° to 7° south latitude
(Figure 2.3). The Borneo Island study area is divided into eight super-regions, with each
super-region comprising of nine sub-regions totally of 72 sub-regions. Sub-regions
were taken such that the centers were detected at sample and lines of widths 105-pixels
(95 km) apart in tile coordinate to enclose all areas of the island.

The same with the New Guinea Island sub-region placement, the Borneo sub-
regions position more land area than water to minimize missing value. Due to the
different shapes of an island, we cannot avoid the water areas to place the sub-regions
for each 72 Borneo's sub-regions distributed equally on the island (Figure 2.3).
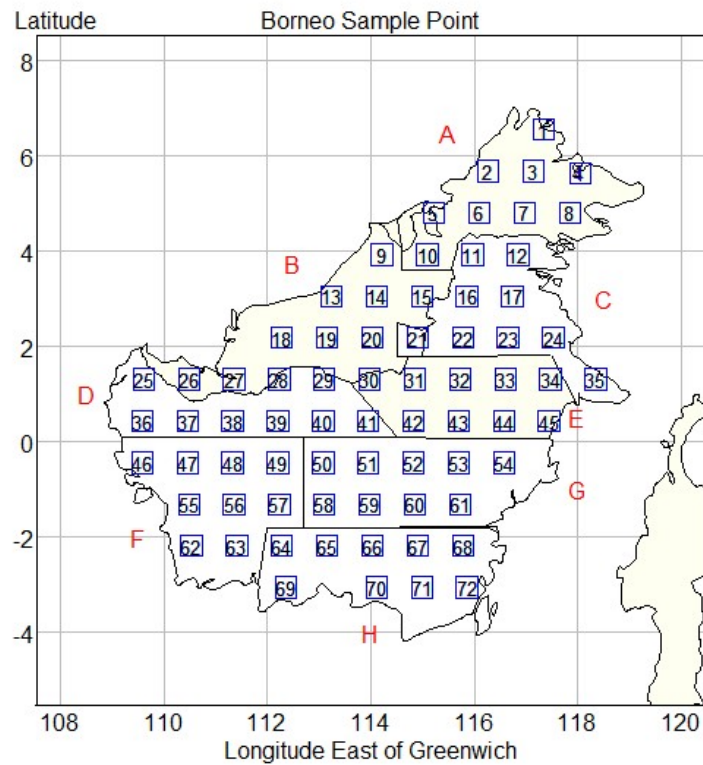
Figure 2.3 Borneo area of study

In Figure 2.3, super-region A represents Sabah & Brunei, super-region B represents Sarawak, super-region C refers to North-Kalimantan, super-region D denotes West-Kalimantan, super-region E refers to East-Kalimantan, super-region F represents West-central Kalimantan, super-region G denotes Central-east Kalimantan, and super-region H represents South-Kalimantan.

The sample of the study is shown in Figure 2.4:
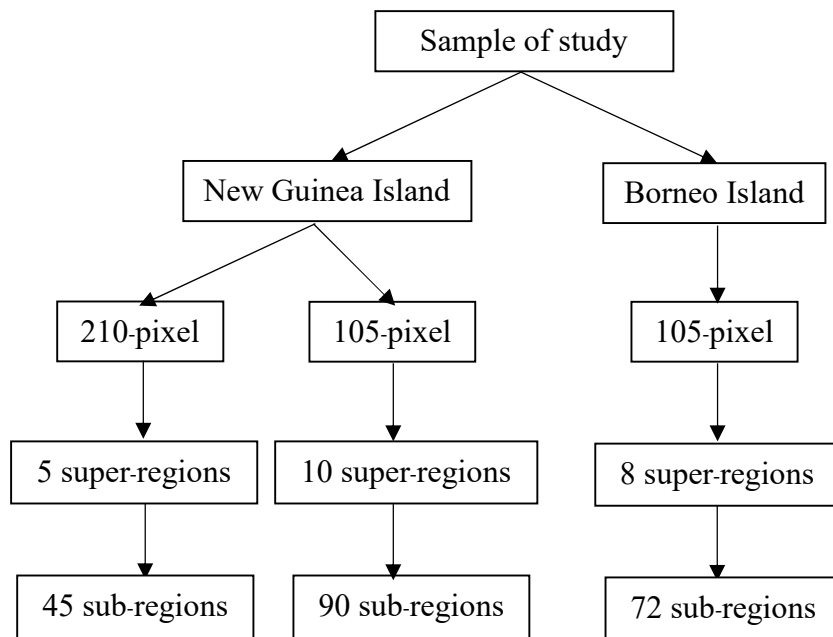
Figure 2.4 Sample of study

New Guinea Island consists of five and ten super-regions that incorporate 45 and 90 sub-regions. Similarly, Borneo Island has eight super-regions and 72 sub-regions (Figure 2.4).

2.2 Data source and data management

Downloaded the LST and NDVI data from MODIS

Data from New Guinea Island and Borneo Island was downloaded using the same procedures. The sub-regions had contrasting land and vegetation characteristics. We used the latitude and longitude of the center point of the sub-region to download the LST and NDVI data from NASA MODIS (DAAC, 2018). The NASA MODIS requires the sub-region central point in geographic coordinated degree (latitude, longitude) to download the data. We have the sub-region coordinate in tile or image coordinate. The tile coordinate's vertical, horizontal, sample, and line values were

transformed into the latitude and longitude coordinates using the MODLAND tile calculator (MODLAND, 2019).

Super-region

The formation of super-regions is shown in Figure 2.5:
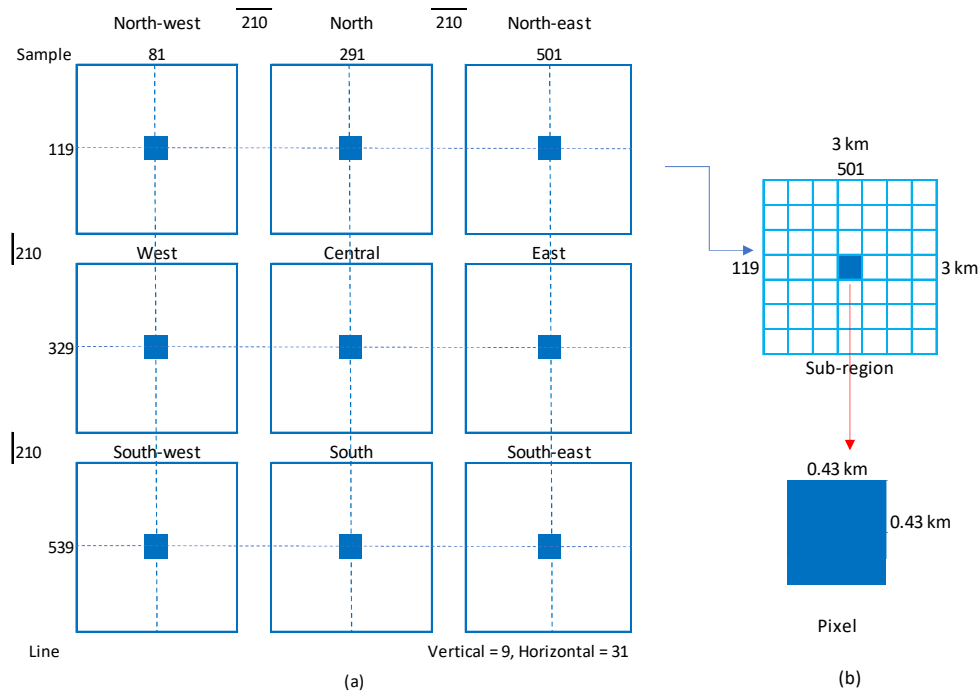
Figure 2.5 Super-region, sub-region, and pixel

Figure 2.5(a); super-region consists of nine sub-regions. The formation of sub-region follows the cardinal and inter-cardinal direction in the nine directions. The blue color square spots the central point of the sub-region. The distance between the central point is 210 sample and line in tile coordinate.

The LST sub-region of New Guinea and Borneo Island has a 3 × 3 km dimension (Figure 2.5(b)). Each sub-region has the data classified into pixels (7 × 7 dimension) with a total of 49 such pixels covering 0.6 equidistant latitude and 0.6 longitude bands, the total sub-region size is 9 km^2, and the dimension for each pixel is approximately 0.184 km^2, as shown in Figure 2.5(b).

We optimized the coverage of the island by adding a sub-region in between two sub-regions. For instance, in the first study area of New Guinea, the sub-regions in super-region A in the tile coordinate with the central point at vertical 9, horizontal 31, line 119, sample 81. These values are rounded values of their coordinates in the sinusoidal projection.
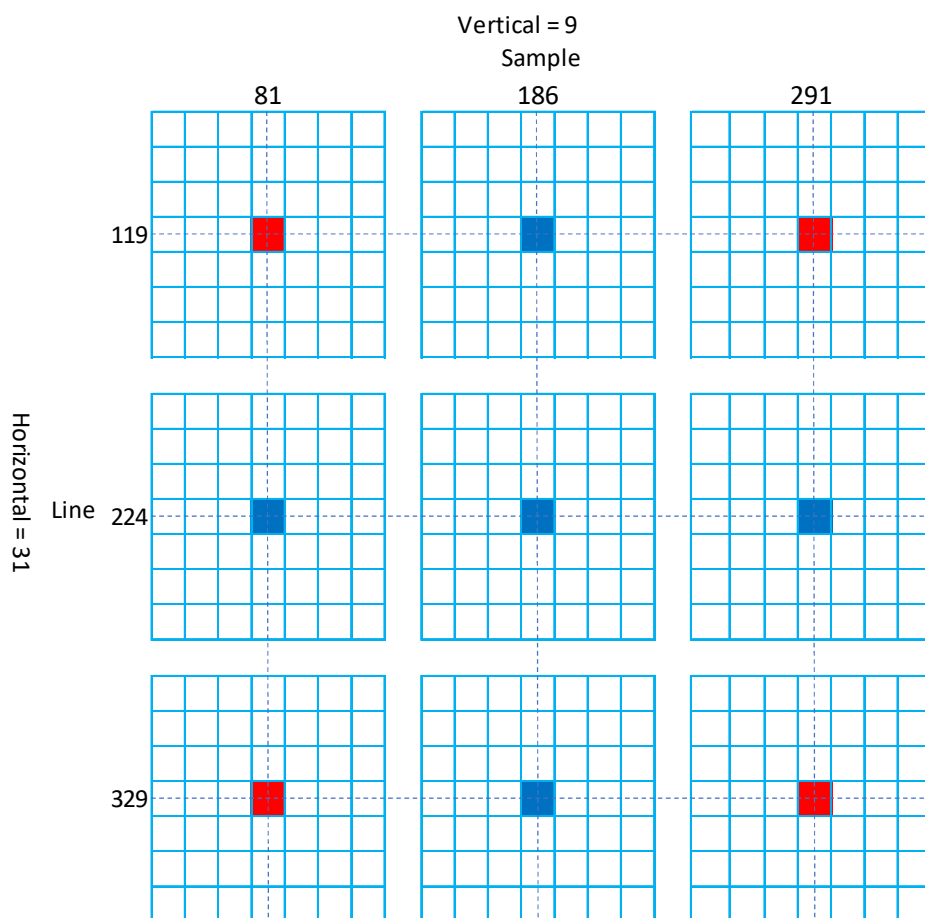
Figure 2.6 Adding the sub-region

Figure 2.6 shows the distance between two red rectangles of the central point is 105 sample and line in tile coordinates with vertical 9 and horizontal 31. We added a new sub-region between 210 samples and line in tiles coordinates, with the center point marked by a blue rectangle. So, the distance between the sub-regions is 105 sample and

line coordinate in tile coordinates, the center points with the rectangle area around 0.43 km^2.

We developed the number of sub-regions if the sub-region did not overlap and remains on the land. For consistency, sub-regions that were identified using different samples should have approximately the same line in tile coordinates. We achieved this result by increasing central sample numbers by 105 samples and line in tile/image coordinate in each successive upper space with various vertical coordinates.

The tile/image coordinate vertical tile = 9, horizon tile = 18, line = -0.50 and sample = -0.50 will have longitude = 0.00 and latitude = 0.00 on the geographic coordinate, in other words the center of the pixel of a tile in the upper left corner has the geographic coordinates (0.0, 0.0). In the upper left corner of the coordinates, tiles are numbered starting with zero. In the integerized sinusoidal, goodes homolosine, and sinusoidal grids coordinate, there are 36 horizontal tiles and 18 vertical tiles. There are 9 horizontal and vertical tiles in the Lambert Azimuthal Equal Area grids. The vertical and horizontal will be changed when the line or sample is more than 1,200-pixels, respectively.

Data download is carried out in overlapping sub-regions. The data were downloaded for every sub-region and then managed to a super-region. For instance, Borneo 1st sub-region of super-region A has vertical = 8, horizontal = 29, line = 412 and sample = 788, transformed into geographical coordinates 117.34 and 6.562 of longitude and latitude (Figure 2.7).
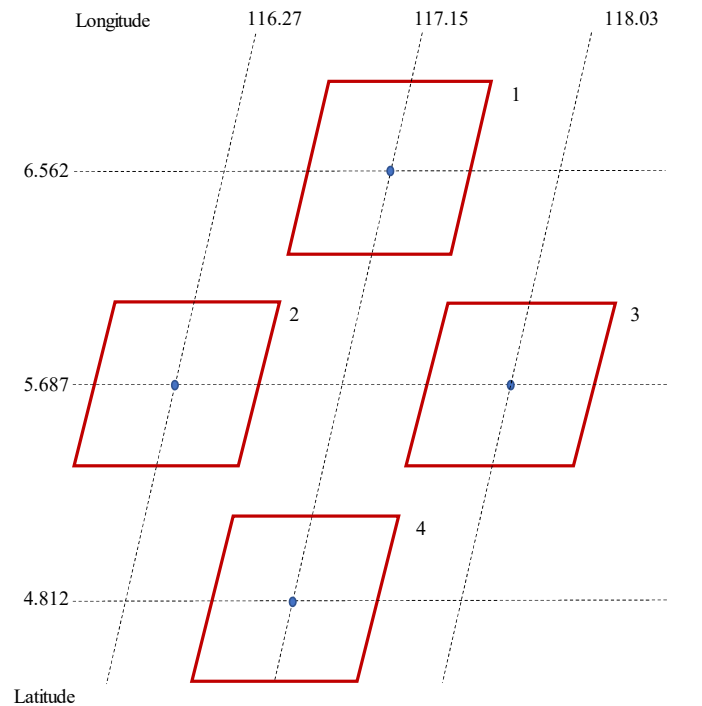
Figure 2.7 Borneo Island sub-region sample point

The selection for the next super-region follows the island shape with the result from the MODLAND tile calculator to avoid overlap between sub-regions. Different from tile or image coordinate, the square change into a trapezoid in geographical coordinate. For example, the sub-region 3 will have 116.27 longitude and 5.687 latitude, then input the longitudes and latitudes (geographic coordinate in degree) on the NASA MODIS web to download the data (Figure 2.7).

We need to adjust the dimension of sub-region size for LST and NDVI for the analysis. We selected a 3 km × 3 km dimension of LST as the trapezoid-shaped sub-region size (Figure 2.8). The smallest trapezoid of NASA MODIS web LST data dimension is 3 km × 3 km. Then, NASA MODIS web will send the desired files and specific coordinate data to the registered email.

We downloaded the Normalized Difference Vegetation Index (NDVI) using the central point of the sub-region with a sub-region dimension of 4 × 4 km, for instance,

the sub-region 1 of Borneo super-region A with 117.34 and 6.562 of longitude and latitude is shown in Figure 2.8 (a). The total size is 1,089-pixels or 33 × 33 pixels, where one pixel is 0.015 km^2. The NASA MODIS NDVI data has a 4 × 4 km dimension of 16 squares with 250 × 250 m. The same with the LST distance between sub-regions, the NDVI sub-region distance was 105 sample and line in tile coordinate.
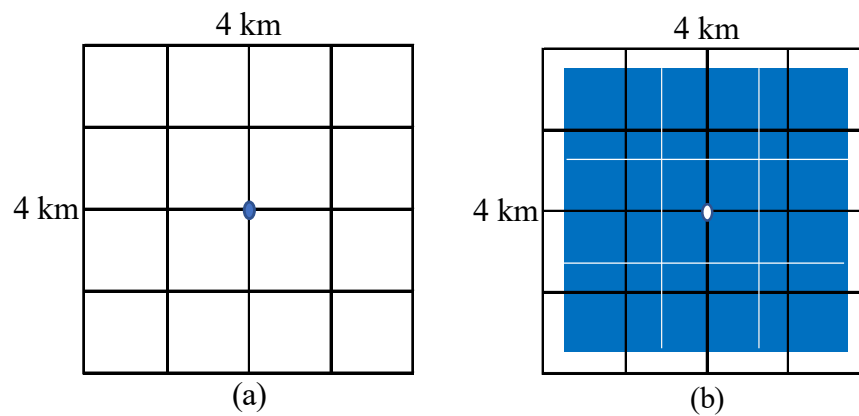
Figure 2.8 NDVI and LST sub-region

Due to the difference of the LST and NDVI sub-region size, we need to ensure that the sub-region central point of the LST and NDVI is identical. Figure 2.8(b) describes the sub-region of LST on the NDVI sub-region, the LST sub-region placed in the central NDVI sub-region is marked by a blue rectangle.

The NDVI data on the NASA web is available every 16 days, and the LST data every eight days throughout the whole year. The NDVI data have 1,089 pixels × 24 days/year × 20 years, and the LST data have 49 pixels × 45 days/year × 20 years or a total of 44,100 data points for each sub-region. The maximum number of LST pixels will have the same number of NDVI pixels after pairing the LST and NDVI data. The NDVI data is also removed from the analysis when the LST data is unavailable on the pixel.

2.3 Variables

The LST variable was used to examine the seasonal pattern and trend on New Guinea and Borneo Island by using the time variable. The LST variable also was used to investigate the correlation with the NDVI variable on Borneo Island.

2.4 Statistical methods

The following statistical methods were employed in this study:

Pearson correlation

The Pearson correlation is a measure of linear association between two variables on an interval or ratio scale. The formula for the correlation coefficient is:

$$r = \frac{\sum(x_i-\bar{x})(y_i-\bar{y})}{\sqrt{\sum(x_i-\bar{x})^2 \sum(y_i-\bar{y})^2}} \tag{2.1}$$

where r is the correlation coefficient between LST and NDVI, x_i is the NDVI as the sample of independent variable values, $\bar{x}$ is the sample mean of NDVI, y_i is the LST as the sample of dependent variable values, and $\bar{y}$ is the sample mean of the LST variable (Rencher and Schaljee, 2008).

Cubic spline

LST seasonal pattern and variation were described using the cubic spline function. The general form of the cubic spline and combination between linear model is:

$$S(t) = a + bt + \sum_{k=1}^{p} c_k(t - t_k)_+^3 \tag{2.2}$$

where $S(t)$ is the spline function (Anton and Rorres, 2010), t denotes the time in days, specified knots are $t_1 < t_2 < ... < t_p$ and $(t - x)_+$ is $(t - x) > 0$ for $t > x$ and 0 otherwise. The boundary conditions require that $s(t)$ for $t < t_1$ equals $s(t)$ for $t > t_p$. a, b, c_k are the

coefficients of the estimator of the cubic spline model. The model becomes a linear model when the cubic spline function has zero knots.

The formula 2.2 derived become the formula 2.3:

$$s(t) = a + bt + \sum_{k=1}^{p-3} c_k \left[(t - t_k)_+^3 - d(t - t_{p-2})_+^3 + e(t - t_{p-1})_+^3 - f(t - t_p)_+^3 \right] \quad (2.3)$$

a, b, c_k, d, e, f are the coefficients of the estimator of the cubic spline model.

LST was seasonally adjusted using the following formula:

$$Y_a = Y - S_f + \bar{y} \quad (2.4)$$

Y_a is a seasonally adjusted time series for LST, Y is a discovered data (day LST) for twenty years, S_f is a vector of spline fitted values evaluated from the cubic splines, and $\bar{y}$ is the mean LST per year. The $\bar{y}$ were added to adjust the LST for seasonal patterns.

Autoregressive (AR)

The autoregressive model is a flexible method for modelling a wide range of time series problems. The formula of the AR(p) model is specified by:

$$Y_t = c + \phi_1 Y_{t-1} + \phi_2 Y_{t-2} + \ldots + \phi_p Y_{t-p} + \varepsilon_t \quad (2.5)$$

where Y_t is the seasonally adjusted LST at time t, and Y_{t-1} is the LST at time t-1, $t =$ time. ϕ_p are unknown parameters to be evaluated, and ε_t is normally distributed or white noise with mean zero and variance one (Hyndman and Athanasopoulos, 2018).

Linear regression

The linear regression model was used to investigate the LST trend. The formula is given by:

$$Y_i = \beta_0 + \beta_1 x_1 + \varepsilon_i \quad (2.6)$$

where Y_i is LST variation for every sub-region as the dependent variable, x_1 is the independent variable, ε_i is the error of the data, β_0 is the intercept for the linear model, and β_1 is the coefficient of the independent variable (Rencher and Schaljee, 2008).

The LST variation for the super-region from each sub-region was examined using the multivariate regression model (Mardia et al., 1979). The model is specified by:

$$\boldsymbol{Y} = \boldsymbol{XB} + \boldsymbol{U} \tag{2.7}$$

$\boldsymbol{Y}$ is the result variables matrix with size $n \times m$, n is the number of the observations, m is the sub-regions number. $\boldsymbol{X}$ is an independent variables matrix $n \times q$, q is the number of the independent variables, $\boldsymbol{B}$ is a matrix of regression parameters with size $q \times m$, and $\boldsymbol{U}$ is a matrix of unobserved random disturbance.

The data analysis and graphical presents were investigated using R (R Core Team, 2017).

2.5 Study diagram

The study diagram explains the data and the statistical methods involved in this study (Figure 2.9):

```
┌─────────────────────────┐
│  Day average LST from 2000│
│         to 2019           │
└─────────────────────────┘
            │
            ▼
┌─────────────────────────┐         ┌───┬─────────────────────────┐
│  LST plot to observe the │◄────────│ 1 │   Cubic spline model    │
│      seasonal pattern     │         └───┴─────────────────────────┘
└─────────────────────────┘
            │
            ▼
┌─────────────────────────┐         ┌─────────────────────────────┐
│      Seasonally LST       │◄────────│   Seasonally adjusted model │
└─────────────────────────┘         └─────────────────────────────┘
            │
            ▼
┌─────────────────────────┐         ┌─────────────────────────────┐
│  LST data independence    │◄────────│        AR(p) model          │
│       examination         │         └─────────────────────────────┘
└─────────────────────────┘
            │                        ┌─────────────────────────────┐
            ▼                   ─────►│   Correlation between LST    │
┌─────────────────────────┐    │     │          and NDVI            │
│ LST variation determination│◄──┘     └─────────────────────────────┘
└─────────────────────────┘
            │                        ┌───┬─────────────────────────┐
            ▼                   ─────►│ 2 │   Cubic spline model    │
┌─────────────────────────┐    │     └───┴─────────────────────────┘
│     LST linear model      │◄───┘
└─────────────────────────┘
            │
            ▼
┌─────────────────────────┐
│  LST multivariate regression│
└─────────────────────────┘
```
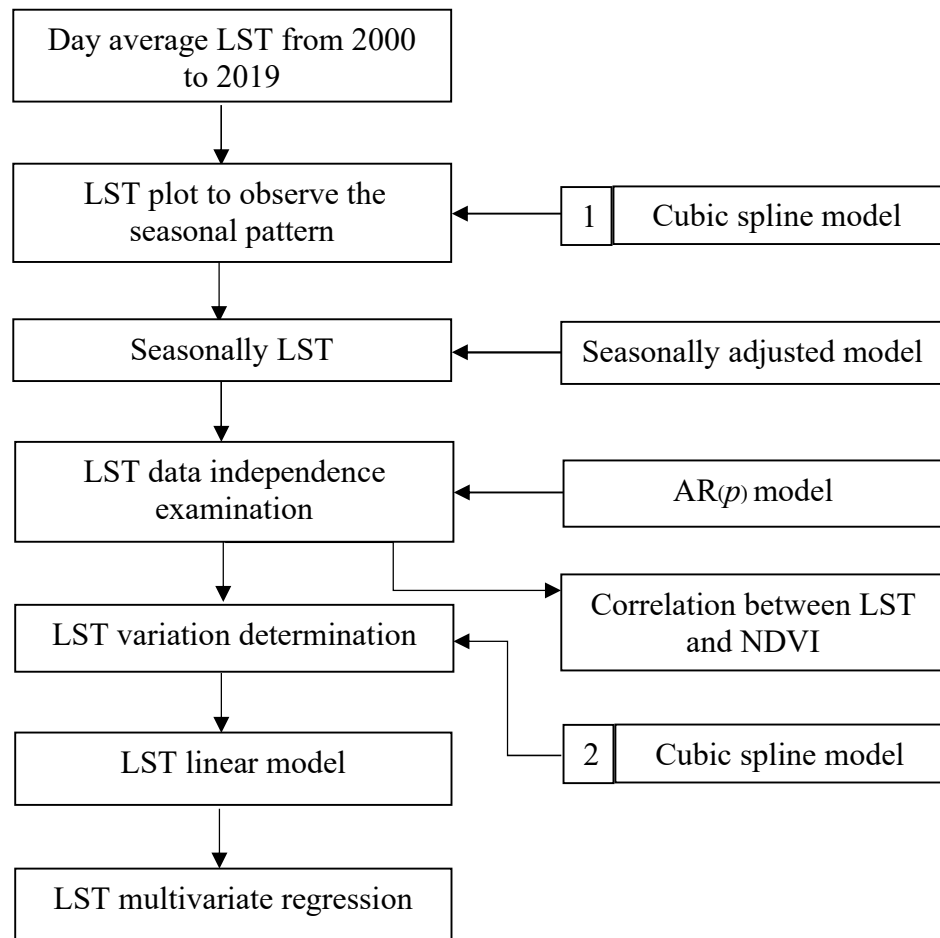
Figure 2.9 LST analysis diagram

Figure 2.9 showed the flow of this research and day average LST from 2000 to 2019 with LST seasonal pattern, variation, and correlation between seasonally adjusted LST and NDVI. The first cubic spline model with eight knots was used to find the seasonal pattern. Seasonally adjusted LST was used to transform the LST data and filtered with AR(p). The second cubic spline with seven knots was utilized to observe the LST variation for every sub-region. Multivariate regression analysis was used to learn the LST variation for every super-region.

Chapter 3

Land Surface Temperatures Variation in New Guinea Island

This chapter describes the result of New Guinea Island in two related analyses. The first analysis consisted of 45 sub-regions (210-pixel distance), and the second analysis consisted of 90 sub-regions (105-pixels distance). The LST variation from different distances compared to have the optimum distance between sub-regions on the island. We have used the cubic spline with the various knots to observe the LST seasonal and the variation patterns from 2000 to 2019. These results also appeared in Munawar et al. (2020).

3.1 First analysis

Super-region A seasonal pattern using a cubic spline model with eight knots (Formula 2.2) was shown as an example super-region in Figure 3.1.
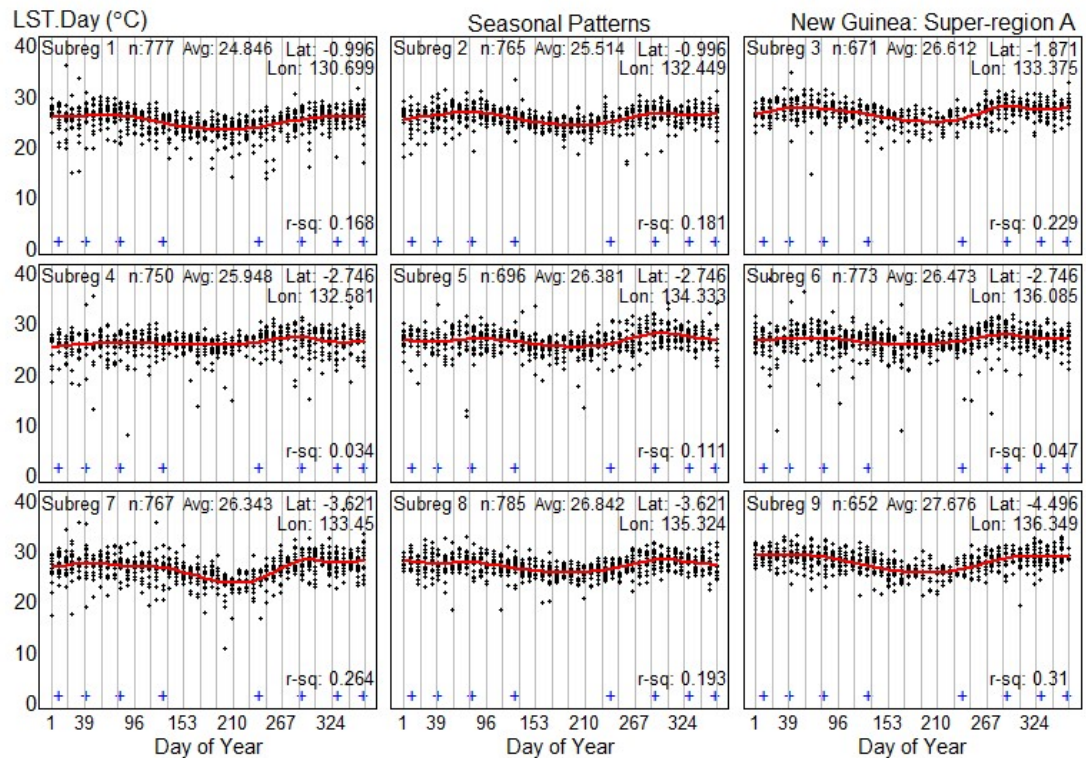
Figure 3.1 New Guinea LST super-region A seasonal pattern

Figure 3.1 showed the seasonal pattern for each sub-region of A super-region with each LST data number, an average of LST, and the latitude and longitude. The vertical axis denotes the average day LST starting from day 1 in January and ending at day 365 in December for 20 years, and the data is marked with a black dot on each day of the year. The red curves are the fitted spline functions with eight knots indicated by blue crosses.

The figure manifested a medium seasonal pattern on super-region A. The lowest LST corresponded to around day 210 (in July) during the rainy season, and the highest LST around day 324 (in November) during the dry season. The highest average day LST was 27.676°C which occurred in sub-region 9 of super-region A with the R-squared was 0.310. The lowest R-squared was 0.034, which happened in sub-region 4 (Figure 3.1).

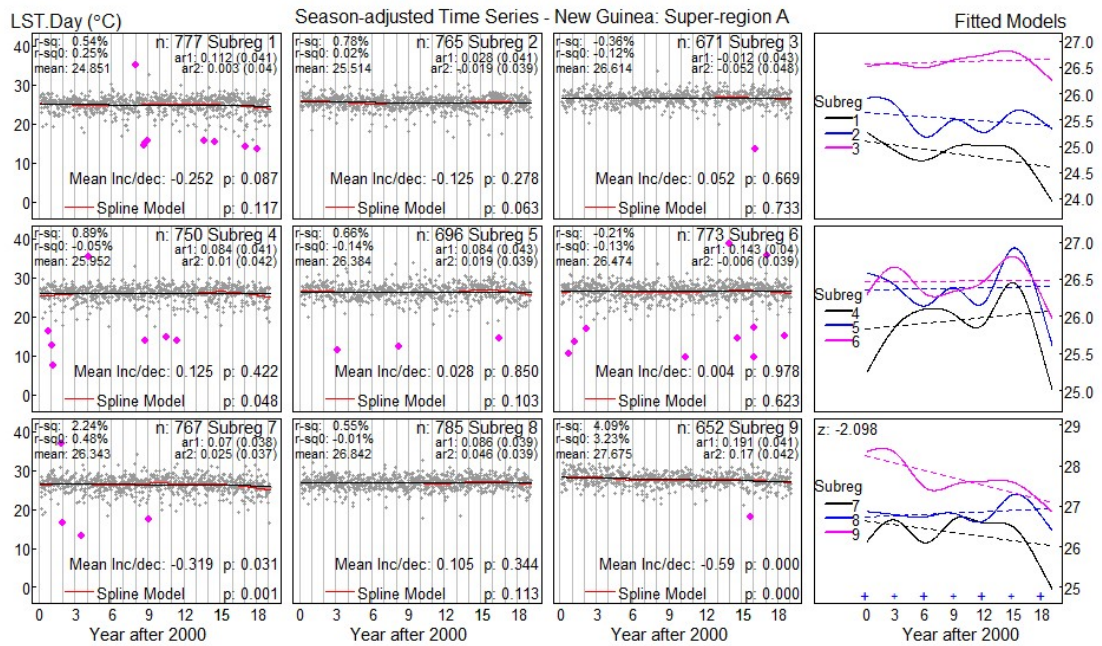Figure 3.2 shows the seasonal adjusted of LST (Formula 2.4).

Figure 3.2 Super-region A seasonally adjusted LST

Figure 3.2 shows the estimated coefficients of autoregressive AR(2) were very low, specifying that the time series of day LST are independent data after adjusted. The dotted lines in the right panel specify that LST decreased in sub-regions 1, 2, 7, and 9, increased in sub-regions 3, 4, and 8, and persisted stable in sub-regions 5 and 6. The p-values for the linear models (zero knots) between Time and adjusted LST marked by a dashed line, none of LST variation was statistically significant. The thick curves in the right panel show a cubic spline with seven knots fitted with significant p-values for sub-regions 4, 7, and 9.

The number and positioning of the knots turn on the LST variation in the year. The seven knots were put in the year interval equally. The z-value of LST variation was -2.098 (Figure 3.2), greater than the critical value of |1.96|. If any z-value less than the absolute of the critical value indicates, there was not a significant variation of LST. The multivariate regression model analyzed the LST variation from the linear model for

every sub-region to narrow spatial correlation and estimate the average of LST for super-region A as an example.

The LST change from the linear model for every sub-region formed into a 95% confident interval in Figure 3.3:
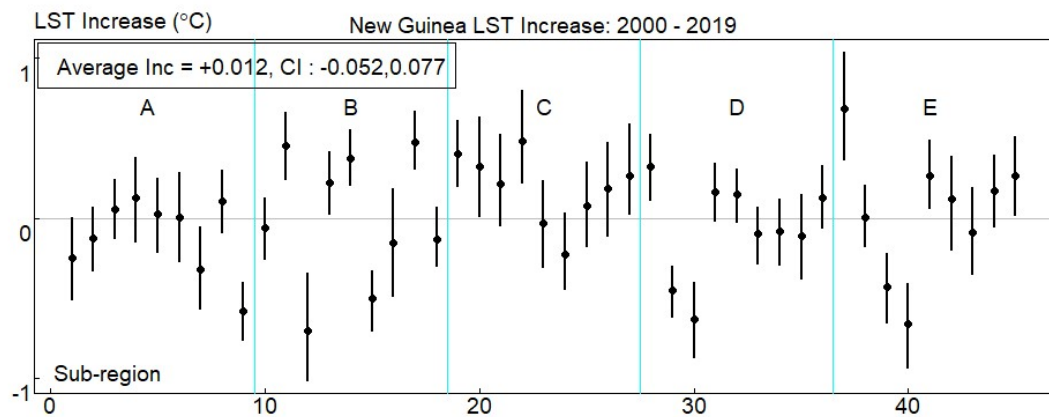
Figure 3.3 The 95% confident interval LST variation for the sub-region

Figure 3.3 shows the variation of LST for each sub-region on the super-region marked by A, B, C, D, and E. The zero line is drawn with the dashed line. If any of the 95% confidence intervals include zero, there was no significant change of LST. The high variation happened in the sub-regions 12 and 37 with a wide confidence interval. The difference varies on the sub-regions without a significant result from -0.052°C to 0.077°C with an average LST increase +0.012°C.

Figure 3.4 shows the variation of LST from the linear and multivariate regression model for super-region A as an example.
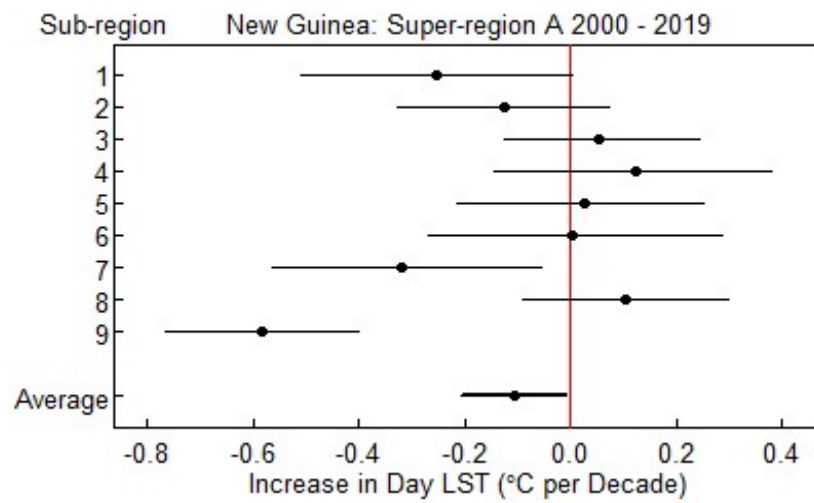
Figure 3.4 The 95% confident interval LST variation for super-region A

Figure 3.4 shows the 95% confidence interval of LST in super-region A. If any of the 95% confidence intervals include zero, there was no significant change of LST. The mean variation of LST was found from the linear model for every sub-region.

Figure 3.4 derived from linear models together with intercepts, coefficients (LST variation), and standard errors for each sub-region in super-region A after seasonal adjusted LST. The result for super-region A (Table 3.1):

Table 3.1 Super-region A linear model coefficients

Sub-region	1	2	3	4	5	6	7	8	9
Intercept	25.09	25.63	26.56	25.83	26.36	26.46	26.64	26.74	28.23
Coefficient	-0.25	-0.12	0.06	0.12	0.02	0.01	-0.31	0.10	-0.58
Standard error	0.13	0.10	0.09	0.13	0.12	0.14	0.13	0.10	0.09

The mean variation of LST for super-region A was obtained from the average of sub-regions linear model coefficient. The average of LST variation for super-region A:

LST variation = (sum of coefficient/number of sub-region)

LST variation = (-0.95/9) = -0.105°C per decade.

The standard error was calculated from sub-regions variance co-variance (Table 3.2):

Table 3.2 Sub-regions variance co-variance

Sub-region	1	2	3	4	5	6	7	8	9
1	**0.017**	0.002	0.001	0.002	0.002	0.002	0.001	0.000	0.001
2	0.002	**0.010**	0.002	0.002	0.001	0.001	0.001	0.001	0.001
3	0.001	0.002	**0.009**	0.001	0.002	0.001	0.002	0.001	0.001
4	0.002	0.002	0.001	**0.018**	0.001	0.001	0.002	-0.000	0.000
5	0.002	0.001	0.002	0.001	**0.014**	0.001	0.002	0.002	0.001
6	0.002	0.001	0.001	0.001	0.001	**0.020**	0.002	0.002	-0.000
7	0.001	0.001	0.002	0.002	0.002	0.002	**0.017**	0.001	0.000
8	0.000	0.001	0.001	-0.000	0.002	0.002	0.001	**0.010**	0.001
9	0.001	0.001	0.001	0.001	0.001	-0.000	0.000	0.001	**0.009**

Table 3.2 showed variance co-variance from the linear models for each sub-region with the variances in the diagonal line of the table marked with bold numeric. The standard error calculation was:

standard error = sqrt (sum variance co-variance)/ (number of sub-region)

standard error = sqrt (0.213)/9 = 0.051°C

The LST variation from the multivariate regression model for every super-region formed into a 95% confidence interval in Figure 3.4:
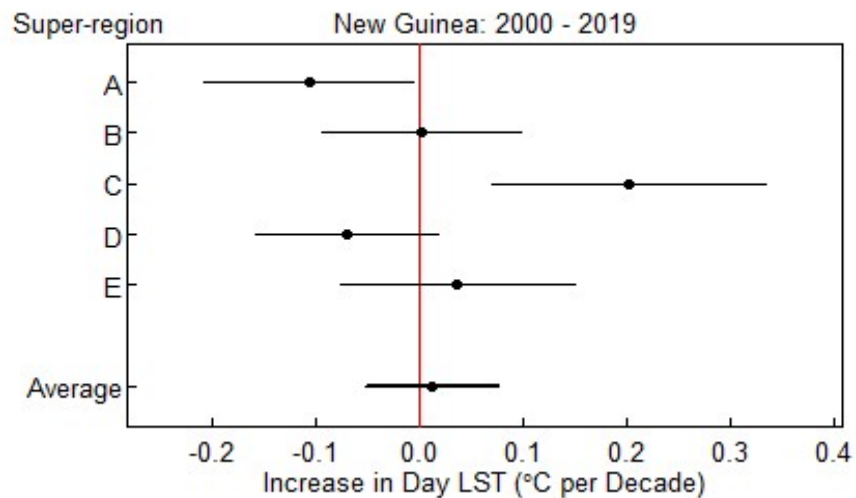
Figure 3.5 Increase in mean day LST with 95% confidence intervals

The rises in LST (°C per decade) for every super-region have appeared in Figure 3.5. There was a wide variation for each super-region, the average change in day LST for the super-region A, B, C, D and E were -0.107°C, 0.002°C, 0.201°C, -0.071°C and 0.037°C, respectively. Only the south and northwest super-regions had significant variations in day LST.

The variation of day LST from the multivariate regression model for every super-region is also explained in the map (Figure 3.6).
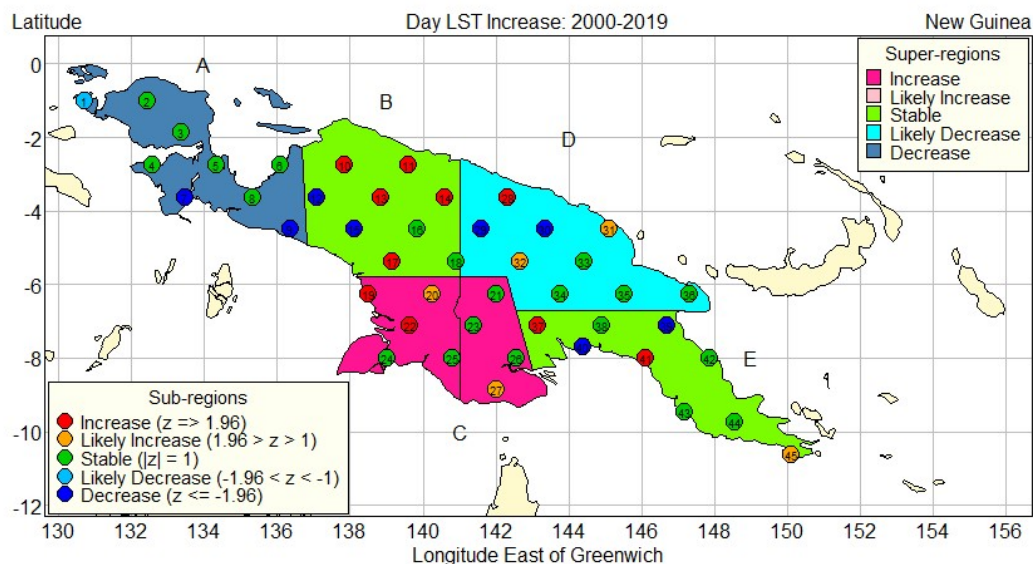
Figure 3.6 The super-region LST variation from 2000-2019 (°C/per decade)

Figure 3.6 manifests the variation of day LST for each super-region on the graphical map. The LST variation decreased on the super-region A (steel blue color), slightly decreased on the super-region D (cyan color), stable on the super-region B and E (lawn green color) and increased on the super-region C (deep pink).

3.2 Second analysis

The super-region A divided into super-region A1 and A2. The same with the first analysis, the seasonal pattern for super-region A1 and A2 using cubic spline model with eight knots was shown as the example regions in Figure 3.7 and 3.8:
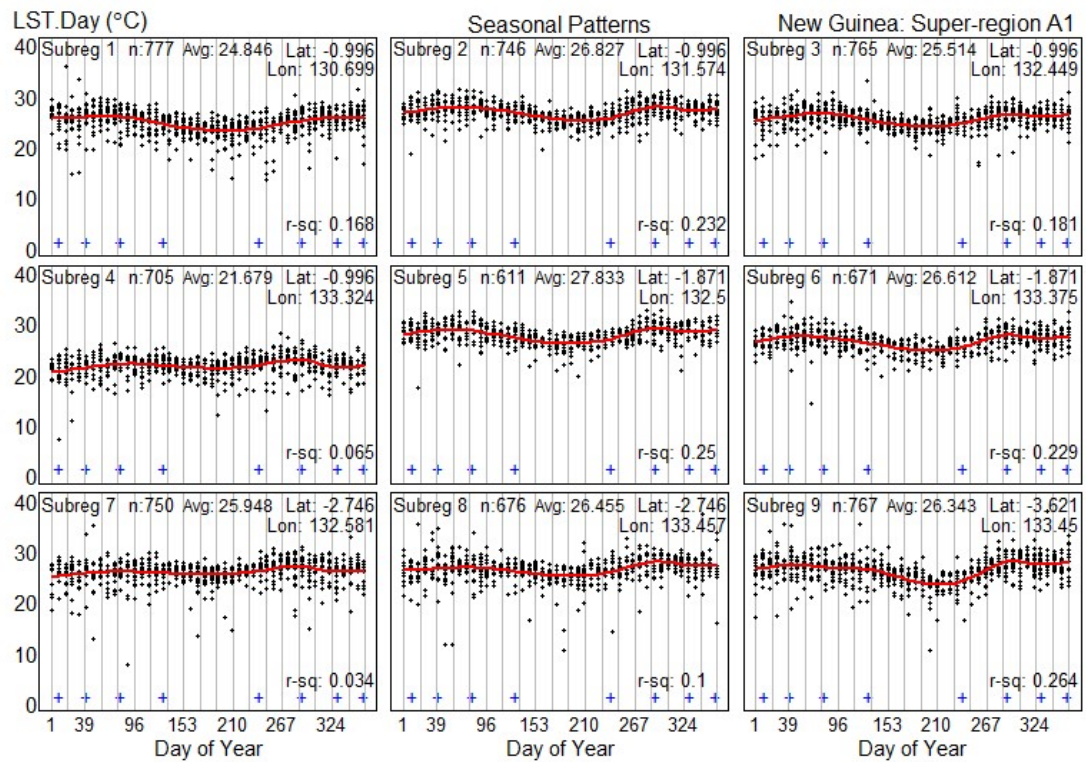
Figure 3.7 Super-region A1 LST seasonal pattern
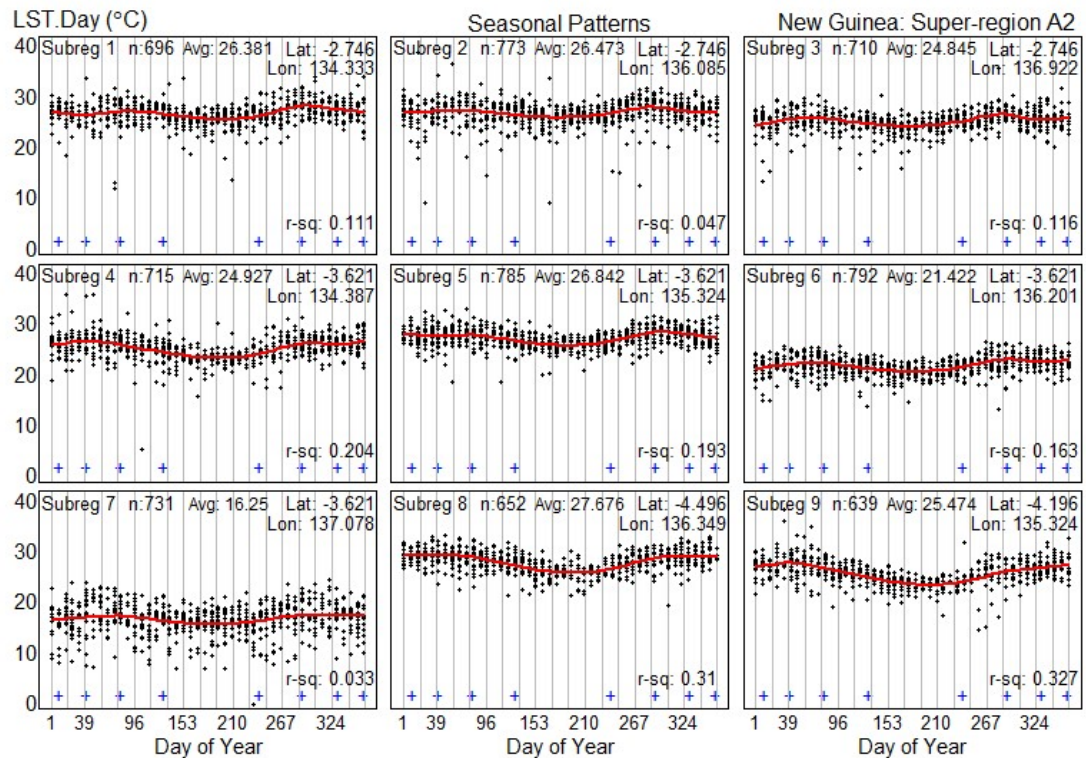
Figure 3.8 Super-region A2 LST seasonal pattern

Figures 3.7 and 3.8 show the seasonal pattern for each sub-region of A1 and A2 super-regions, respectively, with LST data amount (*n*), an average of LST, and the latitude and longitude. The vertical axis denotes the average day LST, and the data is marked with a black dot on each day of the year. The red curves are the fitted natural spline functions with eight knots indicated by blue crosses.

Figure 3.7 shows a moderate seasonal pattern on super-region A1 (north-west1). The minimum LST corresponded to around day 210 (in June) during the rainy season, and the maximum LST around day 324 (in November) during the dry season. The highest mean day LST was 27.833°C, which happened in sub-region 5 of super-region A1 with an R-squared of 0.250. The lowest R-squared was 0.034, which occurred in sub-region 7 (Figure 3.7).

Almost the same as the seasonal pattern of Figure 3.7, Figure 3.8 shows a moderate seasonal pattern on super-region A2 (north-west2). The minimum LST corresponded to around day 210 (in June) during the rainy season, and the maximum LST around day 324 (in November) during the dry season. The highest mean day LST was 27.676ºC which happened in sub-region 8 of super-region A2 with an R-squared of 0.310. The lowest R-squared was 0.033, which happened in sub-region 7 (Figure 3.8).

Figure 3.9 shows the seasonal adjusted of LST (Formula 2.4).
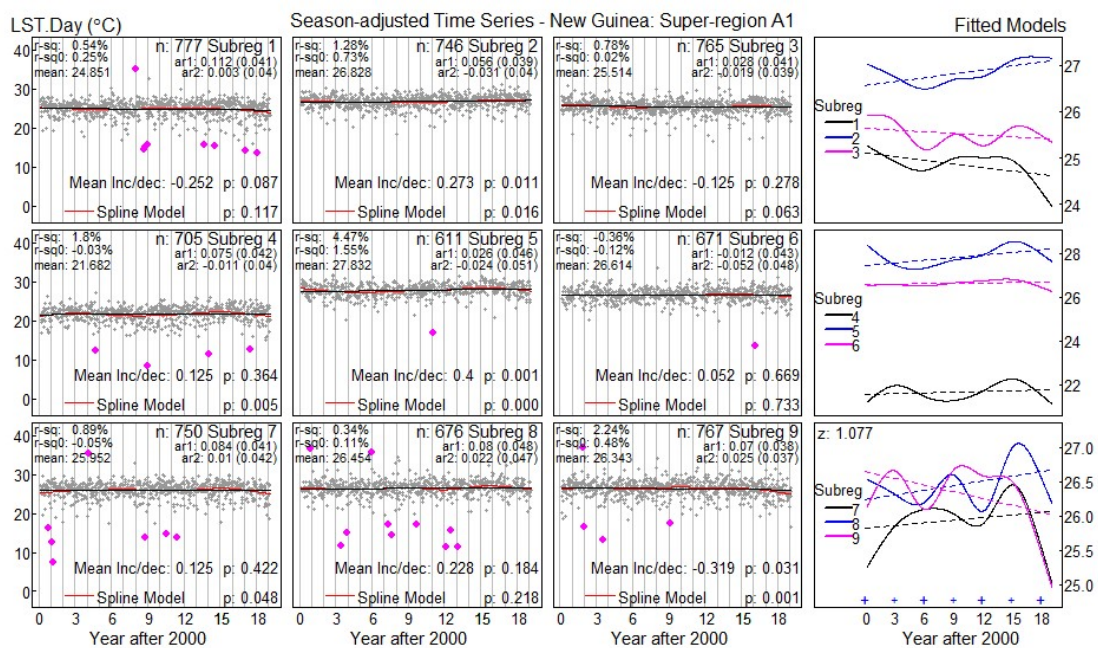
Figure 3.9 Super-region A1 seasonally adjusted LST

Figure 3.9 shows the estimated coefficients of autoregressive AR(2) were very low, specifying that the time series of daily temperatures are independent. The dotted lines in the right panel designate that LST declined in sub-regions 1, 3, and 9, increased in sub-regions 2, 4, 5, 7, and 8, and stable in sub-regions 6 (Figure 3.9). The p-values for the linear models (zero knots) with two parameters designate that sub-region 2, 5, and 9 were statistically significant, indicating a dashed line. The thick curves in the

right panel show fitted cubic splines with seven knots (with significant p-values for sub-regions 2, 4, 5, 7, and 9).

The z-value is 1.077 lower than the critical value of |1.96|, showing a not statistically significant increase of LST (Figure 3.9).

Figures 3.10 shows the seasonal adjusted of LST (Formula 2.4).
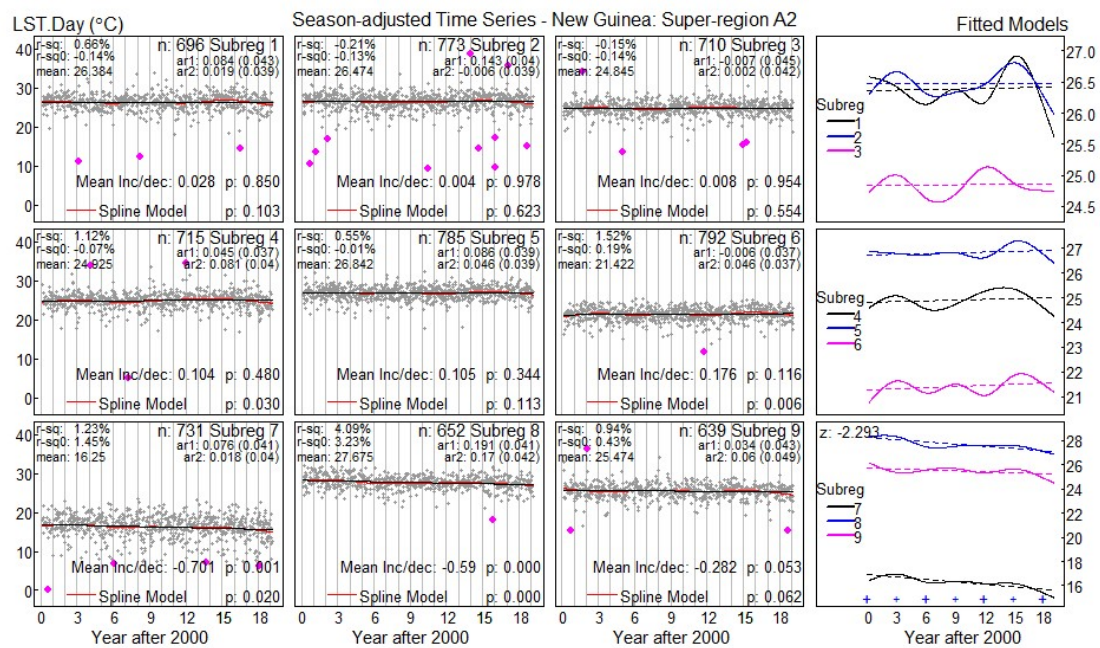
Figure 3.10 Super-region A2 seasonally adjusted LST

Almost the same with Figure 3.9, Figure 3.10 shows the estimated coefficients of autoregressive AR(2) were very low, specifying that the time series of daily temperatures are independent. The dotted lines in the right panel indicate that LST decreased in sub-regions 7, 8, and 9, increased in sub-regions 5, 6, and 7, and remained stable in sub-regions 1, 2, and 3 (Figure 3.10). The p-values for the linear models (zero knots) marked a dashed line with Time and LST variables indicate that sub-regions 7 and 8 were statistically significant. The thick curves in the right panel show fitted cubic splines with seven knots (with significant p-values for sub-regions 4, 6, 7, and 8).

The z-value is -2.293 greater than the critical value of |1.96|, indicating a statistically significant decrease of LST.

Figure 3.11 shows the LST change for every sub-region formed into a 95% confidence interval.
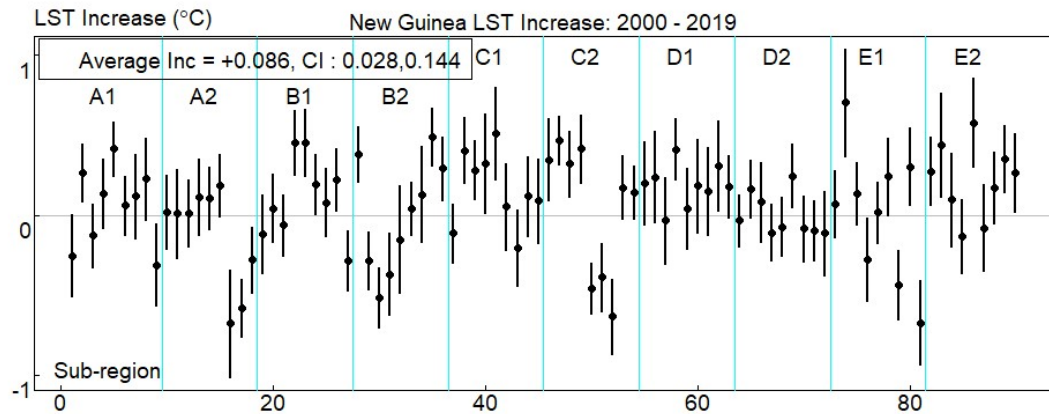
Figure 3.11 The 95% confidence interval of LST for sub-regions

Figure 3.11 shows the variation of LST for each sub-region on the super-region marked by A1 to E2. The zero line is drawn with the dashed line. If any of the 95% confidence intervals include zero, there was no significant change of LST. The LST variation average is +0.086°C per decade with a significant of 95% confidence interval (0.028, 0.144)°C. The sub-regions 16 and 74 have a wide variation of LST.

The LST variation from each sub-region formed into a 95% confidence interval for every super-region described in Figure 3.12:
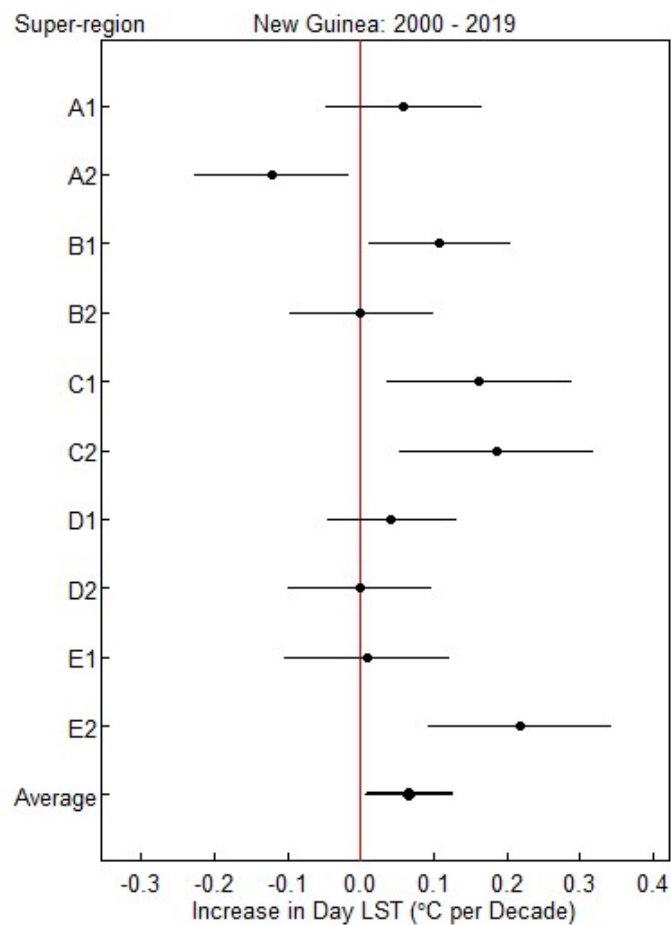
Figure 3.12 Increase in mean day LST with 95% confidence intervals

Figure 3.12 shows the 95% confidence interval of LST mean variation for every super-region. With the total ten super-regions, only super-region A2 (north-west2) has a significant LST decrease, and super-regions B1 (central-north1), C1 (central-south1), D1 (north-east1), and E2 (south-east2) have significantly increased LST. The rest five of super-region has no significant LST variation.

The variation of day LST from the multivariate regression is also explained in the map for each super-region:
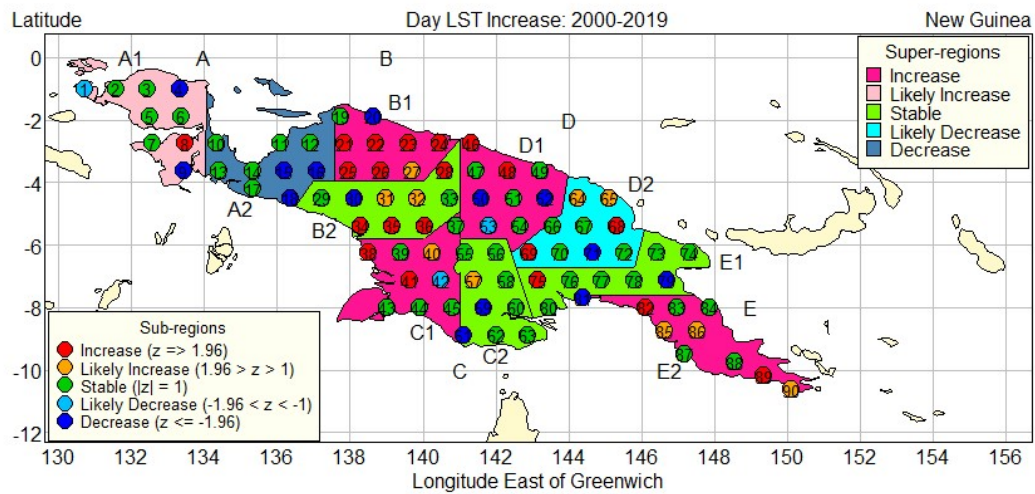
Figure 3.13 Super-region LST increase from 2000-2019 (°C/per decade)

The results of LST variation for each super-region, A2 super-region has a steel blue color (decreased), D2 super-region has a cyan color (likely decreased). B2, C2, and E1 super-regions have lawn green color (stable), A1 super-region has a pink color (likely increased), and the rest super-regions have a deep pink color that indicates the increase of LST (Figure 3.13).

Figure 3.14 shows the comparison of LST variation between 45 sub-regions and 90 sub-regions distance in a 95% confidence interval for every super-region:
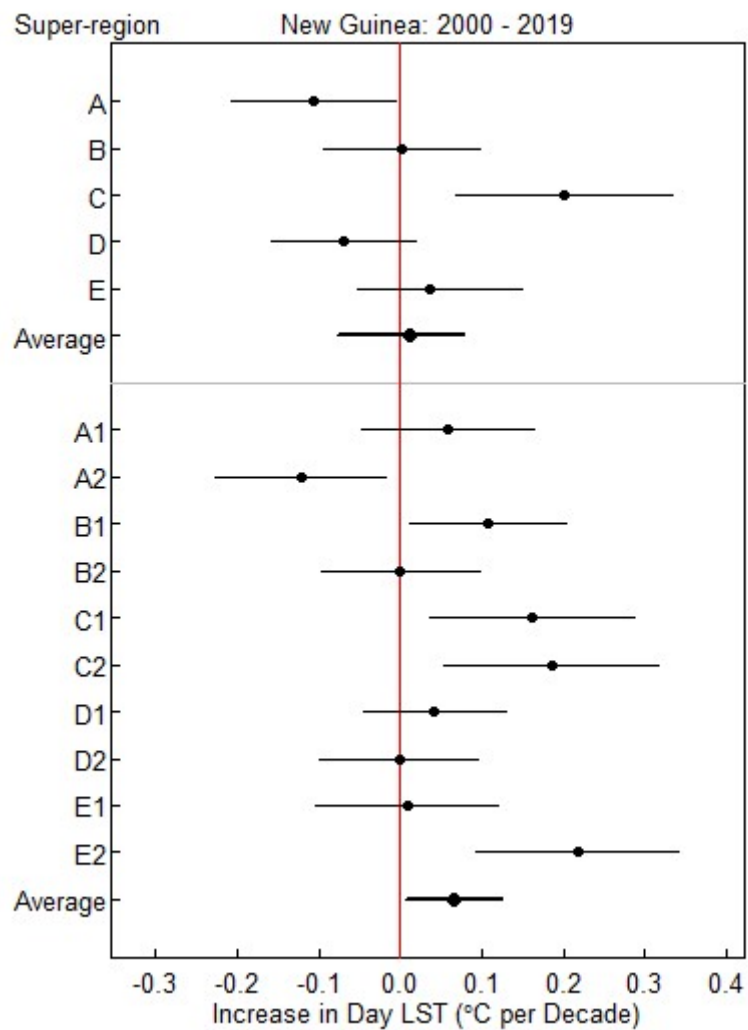
Figure 3.14 New Guinea increases in Day LST confidence interval comparison

Figure 3.14 shows the different results for LST with 45 sub-regions and 90 sub-regions. The five super-regions with 45 sub-regions have not significant 95% confidence interval with an average +0.012 (-0.052, 0.077), while the mean increase of LST for the ten super-regions with 90 sub-regions is +0.086°C per decade with a significant confidence interval (0.028, 0.144). Suppose the confident interval includes the zero-value increase considered a not significant variation of LST.

Figure 3.14 also shows the five super-regions with 45 sub-regions have only one significant confidence interval for super-region C. In comparison, the four super-regions have no significant result of LST variation. The ten super-regions with 90 sub-regions have five super-regions with significant mean variation of LST, super-region A2, B1, C1, D1, E2, and the other five super-regions have no significant increase or decrease LST.

Chapter 4

Land Surface Temperature and NDVI Variation in Borneo Island

This chapter describes the results of Borneo Island on LST variation with eight super-regions consisting of 72 sub-regions. The cubic spline model with the various knots was used to observe the seasonal pattern and variation of LST from 2000 to 2019. The results also appeared in Munawar et al. (2022). This chapter also examines the correlation between LST and NDVI.

4.1 LST variation

The seasonal pattern for super-region A using cubic spline model with eight knots was shown as an example super-region in Figure 4.1:
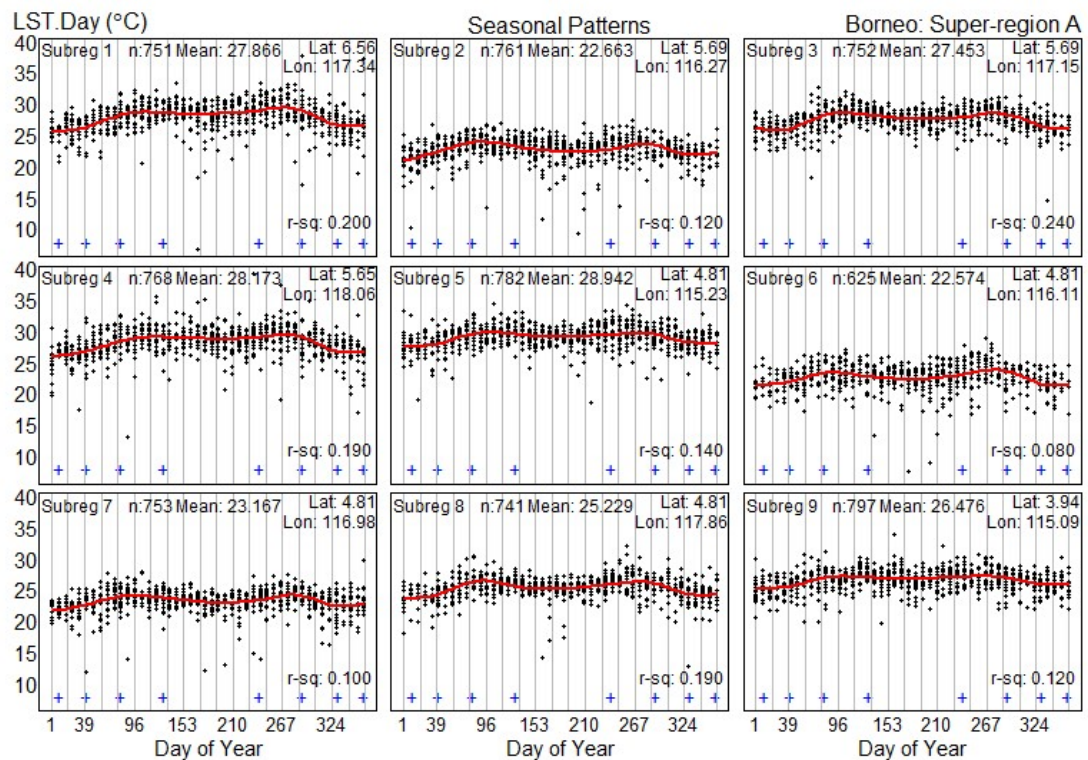
Figure 4.1 Borneo LST super-region A seasonal pattern

Figure 4.1 shows the data approximately fitted natural spline functions with eight knots with solid red curves, indicated by the blue crosses. The figure showed a moderate seasonal pattern on super-region A draws with two summer peaks in March and September throughout the years.

The minimum LST corresponded to around day 1 (in January), and the maximum LST reached around day 267 (September). The highest mean of day LST was 28.942°C which happened in sub-region five of super-region A, and the lowest average of LST was 22.574 in sub-region 6. The highest R-square is 0.200 on the sub-region 1 and the lowest 0.080 on sub-region 6 of super-region A (Figure 4.1).

Figure 4.2 shows the seasonal adjusted of LST.
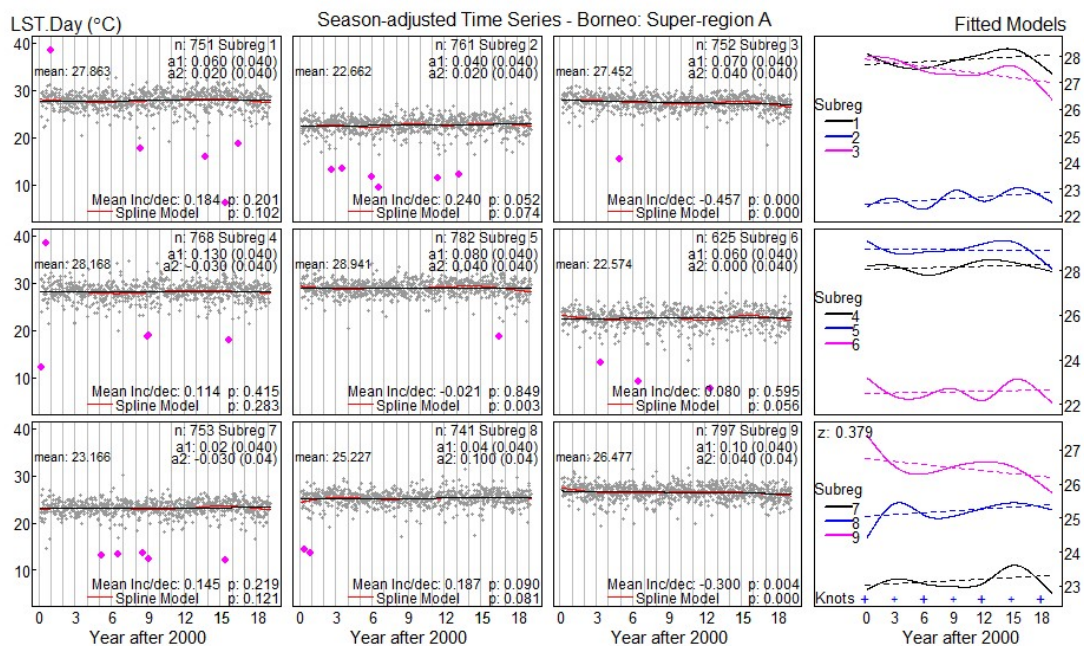
Figure 4.2 Super-region A seasonally adjusted LST

Figure 4.2 shows the estimated coefficients of autoregressive AR(2) was very low, specifying that the time series of daily temperatures are independent. The dotted lines in the right panel indicate that LST decreased in sub-regions 3, 5, and 9, increased in sub-regions 1, 2, 4, 7, and 8, and remained stable in sub-region 6. The p-values for

the linear models (zero knots) with two parameters specify that none of these changes was statistically significant, indicating a dashed line. The thick curves in the right panel show fitted cubic splines with seven knots (with significant p-values for sub-regions 4, 7, and 9).

The number and positioning of the knots depend on the LST variation in the year. The seven knots were put in the year interval equally. The z-value of LST variation was 0.379 lower than the critical value of |1.96|. The multivariate regression model analyzed the LST variation from the linear model for every sub-region to reduce spatial correlation and estimate the average of LST for super-region A as an example.

The LST change for every sub-region formed into a 95% confident interval in Figure 4.3:
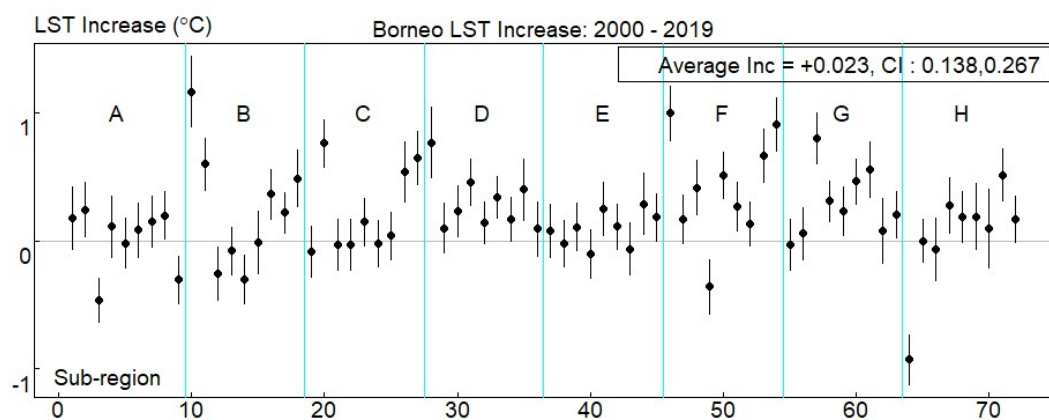
Figure 4.3 The 95% confident interval LST variation for the sub-region

Figure 4.3 shows the increase of the LST average for every sub-region. The zero line is marked with the dashed line. If any of 95% confidence intervals include zero indicated, there was no significant change of LST. The high variation happened in sub-regions 10, 28, and 64 with wide the confidence interval. The difference fluctuated significantly from 0.138°C to 0.267°C with an average increase of +0.023°C.

The LST variation from each sub-region formed into a 95% confidence interval for every super-region described in Figure 4.4:
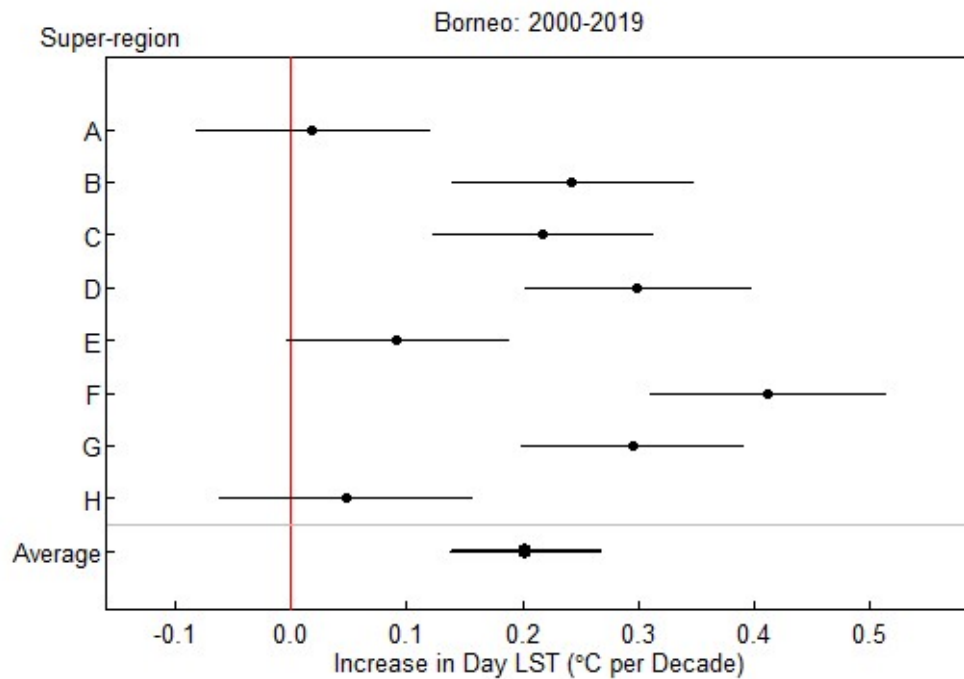
Figure 4.4 The 95% confidence intervals for the mean increase

The mean variation in day LST for super-region A (Sabah and Brunei), B (Sarawak), C (North Kalimantan), D (West Kalimantan), E (East Kalimantan), F (West Central Kalimantan), G (Central Kalimantan), and H (South Kalimantan) were 0.019, 0.243, 0.217, 0.299, 0.092, 0.411, 0.295 and 0.048°C, respectively (Figure 4.4). Five super-regions have a significant mean increase of LST, except three super-region such as A (Sabah and Brunei), E (East Kalimantan), and H (South Kalimantan), which have no significant day LST change.

The variation of day LST from the multivariate regression is also explained in the map for each super-region:
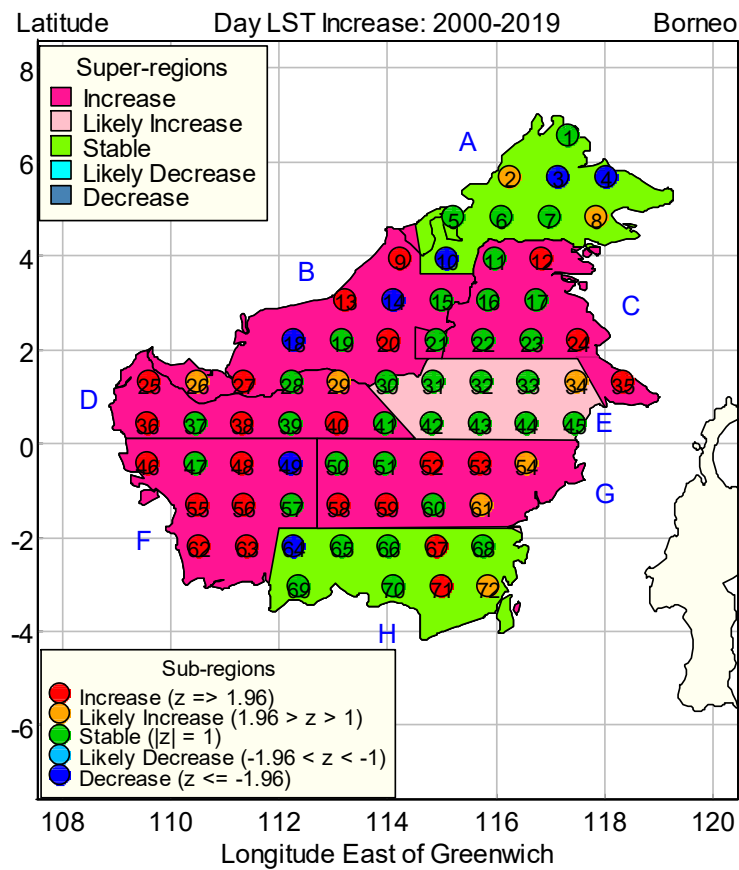
Figure 4.5 Trends in LST for Borneo, 2000 – 2019 ($^\circ$C/decade)

Figure 4.5 exhibits the outcomes of LST variation for eight super-regions with 72 sub-regions with a different color in Borneo Island. We have colored these 72 sub-regions using five colors, signifying the increase or decrease in LST. The super-region A (Sabah and Brunei) had a medium decline in daily LST, B (Sarawak), C (North Kalimantan), D (West Kalimantan), F (West-central Kalimantan), and G (Central Kalimantan) had a rise in LST. At the same time, there was a slight increase in super-region E (East Kalimantan) and H (South Kalimantan).

4.2 Correlation between the LST and NDVI

The correlation between the seasonally adjusted LST and NDVI was investigated using the scatter plot and the Pearson correlation coefficients for super-region A as an example super-region in Figure 4.6 (Formula 2.1).
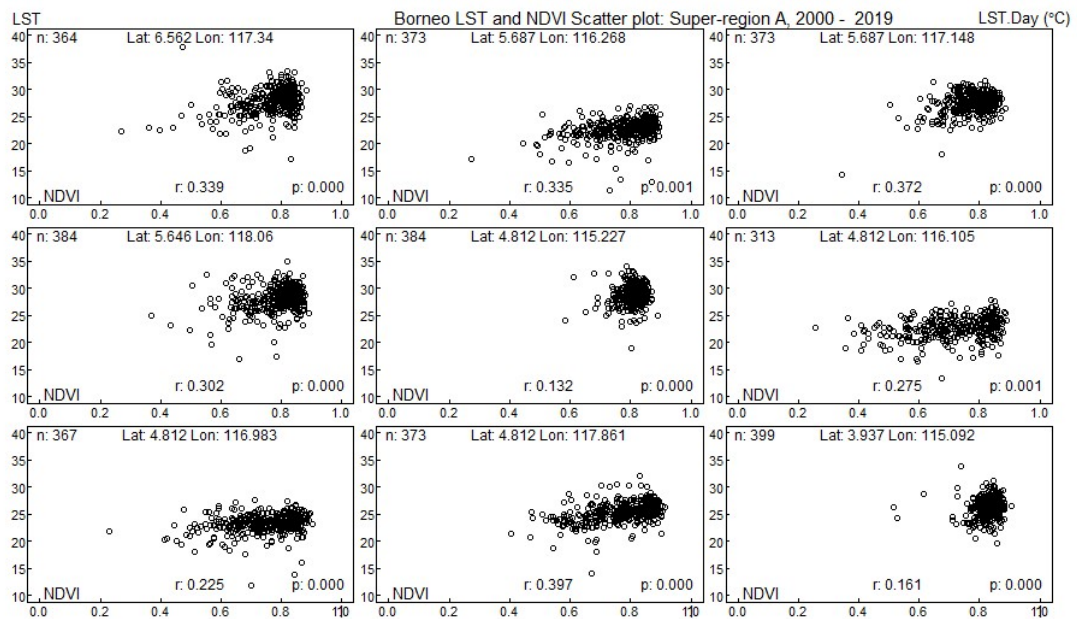
Figure 4.6 Super-region A LST and NDVI correlation

Figure 4.6 shows the amount of LST and NDVI pair data, correlation coefficient, the p-value of the correlation coefficient, and the scatter plot for every sub-region of super-region A. The LST and NDVI scatter plots show a random pattern or do not form a linear pattern indicated with a low correlation coefficients value (r). All correlation coefficients between LST and NDVI are low with a statistically significant. The lowest value of r is 0.132 (p-value: 0.000) with the null hypothesis there is no correlation between LST and NDVI in sub-region 5, and the highest value of r is 0.397 (p-value = 0.000) with the null hypothesis there is no correlation between LST and NDVI in sub-region 8 (Figure 4.6).

Table 4.1 shows the correlation coefficient between LST and NDVI for all super-region on Borneo Island:

Table 4.1 Coefficient correlation of LST and NDVI

Super-region	Sub-region	n	r	p-value	Super-region	Sub-region	n	r	p-value
A	1	364	0.339	0.000	E	30	362	0.338	0.000
	2	373	0.335	0.001		31	257	0.206	0.253
	3	373	0.372	0.000		32	331	0.159	0.001
	4	384	0.302	0.000		33	363	0.267	0.000
	5	384	0.132	0.000		34	320	0.257	0.001
	6	313	0.275	0.001		42	344	0.186	0.000
	7	367	0.225	0.000		43	324	0.156	0.071
	8	373	0.397	0.000		44	258	0.028	0.034
	10	399	0.161	0.000		45	275	-0.035	0.027
B	9	317	-0.285	0.000	F	46	337	0.098	0.000
	13	337	0.162	0.000		47	345	0.098	0.000
	14	370	0.148	0.001		48	293	0.162	0.000
	15	390	0.384	0.000		49	305	0.011	0.000
	18	324	0.201	0.000		55	346	0.234	0.000
	19	345	0.377	0.000		56	344	0.193	0.194
	20	365	0.132	0.000		57	315	0.286	0.006
	26	298	0.209	0.000		62	308	-0.141	0.000
	27	343	0.185	0.000		63	311	-0.101	0.000
C	11	370	0.424	0.000	G	50	317	0.331	0.000
	12	341	0.107	0.577		51	260	0.181	0.001
	16	364	0.295	0.000		52	274	0.042	0.072
	17	250	0.192	0.000		53	268	0.064	0.023
	21	350	0.337	0.000		54	276	-0.072	0.007
	22	335	0.296	0.083		58	279	0.207	0.336
	23	353	0.335	0.000		59	299	0.153	0.009
	24	370	0.211	0.000		60	354	0.265	0.000
	35	307	0.303	0.000		61	317	0.033	0.000
D	25	315	-0.377	0.002	H	64	306	-0.105	0.000
	28	277	0.194	0.000		65	292	0.115	0.000
	29	335	0.209	0.000		66	349	0.149	0.000
	36	330	0.222	0.000		67	340	0.145	0.000
	37	289	0.177	0.000		68	323	0.084	0.000
	38	224	0.08	0.000		69	355	-0.177	0.000
	39	262	0.133	0.000		70	351	-0.121	0.000
	40	305	0.224	0.000		71	301	-0.318	0.000
	41	343	0.189	0.000		72	349	0.005	0.000

Table 4.1 shows the variation of the correlation coefficient between LST and NDVI for every sub-region of Borneo Island. The missing value or unpaired LST and NDVI were removed for 72 sub-regions ranging, the number of data ranging from 224 to 399. The sub-regions have low and statistically significant correlation coefficients varying from -0.377 to 0.424. The correlation coefficient of Borneo Island has a positive correlation coefficient indicating that if LST increases, the NDVI also increases. The sub-regions of super-regions B, D, E, F, G and H have a negative correlation coefficient. Mainly super-region H in the south of Borneo Island has a negative correlation coefficient with a stable LST variation.

The Pearson correlation coefficients were low. The scatter plot pattern is random or does not form a linear pattern. The cubic spline model was used to examine pattern of LST and NDVI. Figure 4.7 shows the LST and NDVI using the formula 2.3 with eight knots for super-region A as a sample super-region:
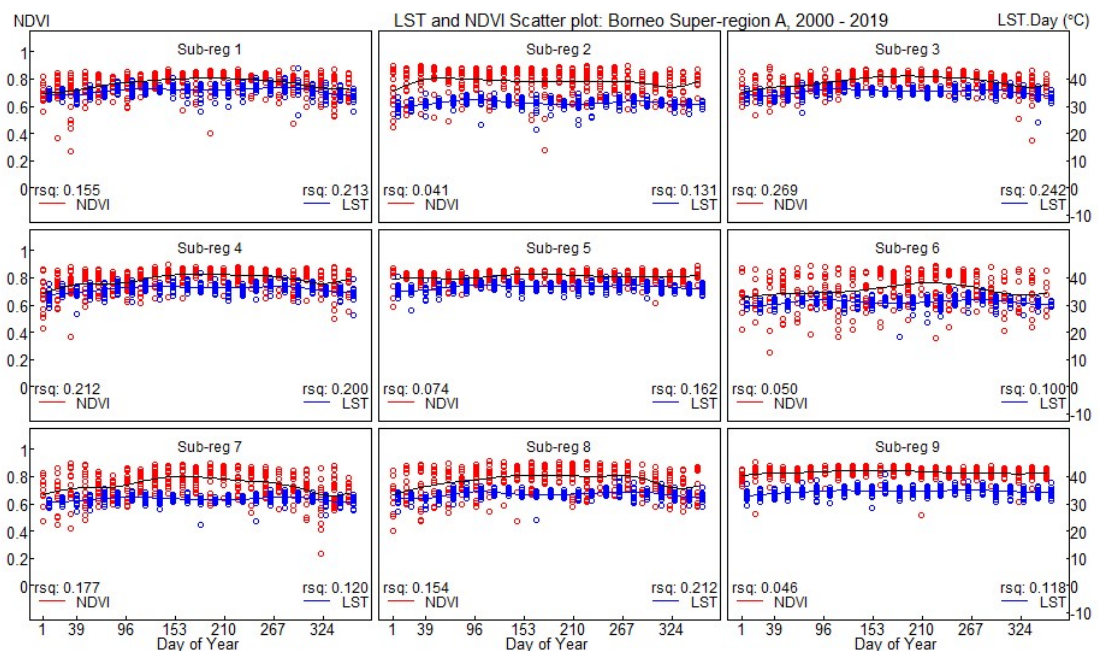
Figure 4.7 LST and NDVI pattern

Figure 4.7 shows LST data marked with a blue dot and NDVI data with a red dot, and the blue line is the cubic spline model for LST and the red line for the NDVI model.

Figure 4.7 also shows the LST and NDVI pattern for every sub-region of super-region A, which displayed two patterns of LST and NDVI. The sub-regions 2, 5, and 9 have increased from around day 1 (in January) to around day 113 (in April). Flat together from around day 113 (in April) to around day 337 (in December). The pattern slightly increases together from around day 337 to the end of the year. The rest of the sub-regions have increased together in the beginning, away from each other in the middle, and slightly increased together at the end of the year. The highest R-square of LST is 0.242, and the R-square of NDVI is 0.269 in sub-region 3, the lowest R-square of LST is 0.118, and the R-square of NDVI is 0.046 in sub-region 9.

Chapter 5

Discussion and conclusion

This chapter summarises the findings on the LST variation result on New Guinea and Borneo Island and the correlation between LST and NDVI on Borneo Island. The limitation and recommendations of this research are also discussed.

5.1 Discussion

The New Guinea Island was divided into two areas of analysis. The first analysis consisted of 45 sub-regions (210-pixels distance), and the second analysis consisted of 90 sub-regions (105-pixels) on the island. The seasonal pattern of LST was found on the New Guinea Island at 45 sub-regions and 90 sub-regions. The lowest LST corresponded to the rainy season, and the highest LST dry season. The seasonal pattern on the island is influenced by southeast trade, monsoon, and the characteristic of the island, such as latitude, elevation, and exposure (Jackson and Standish, 2019).

The overall mean increase of LST per decade for 45 sub-regions was $+0.012^{\circ}C$, the confidence interval was $(-0.052, 0.077)^{\circ}C$. The 90 sub-regions had a significant overall mean increase of LST $+0.086^{\circ}C$, with the confidence interval being $(0.028, 0.144)^{\circ}C$. The result on 90 sub-regions was similar to the finding in Milne Bay province of New Guinea Island with a positive trend of sea surface temperature $0.09^{\circ}C$ per decade for 40 years ago (Davies and Brown, 1997).

The first analysis the result show that there were two super-regions A (north-west) and C (central-south) that had significant mean decrease and increase of LST with $-0.107^{\circ}C$ and $0.201^{\circ}C$ respectively. The second analysis had five super-regions with

significant mean variation of LST. There were four super-regions with the mean LST increase in B1 (central-north1), C1 (central-south1), C2 (central-south2) and E2 (south-east2) with 0.008°C, 0.042°C, 0.185°C, 0.217°C, respectively, and one of super-region of A2 (north-west2) has mean LST decrease by -0.122°C. The rest five super-region has no significant LST variation. The addition of the sub-regions or reduced distance between sub-regions on New Guinea Island did not increase the spatial correlation. The opposite with the research on Europe and North America air temperature records, the spatial correlation will increase not only by the station's distance but also by the continentality of the stations or the climate condition (Malcher and Schönwiese, 1987).

The increase in LST on the island indicated climate change because it was part of frequent weather change (Ayuningtyas, 2015). LST changes because it was influenced by urbanization LU/LC change (such as forest degradation and deforestation) (Fu and Weng, 2016). The greater levels of human activities that do not care for the environment can cause global warming, mainly because of reduced rainforest or green open space. Warming could occur on the island because of increased LST. Also, the increase in LST can be used as an indicator of heat islands, one of the causes of warmer LST. Heat islands can impact heatwaves, which affect the quality of life and the environment.

A study reveals on the drought in Papua New Guinea that is related to LST and NDVI, and it was found that there was a risk zone, especially in the Western Highlands province (Korada et al., 2018). Based on that study, LST indicates drought from radiation levels. When radiation is high, there is little water content at the surface of the soil. Deficiency occurs because the temperature is too high, causing the water in the ground to evaporate.

The LST in Borneo Island also showed a similar seasonal pattern with the New Guinea Island. The lowest LST corresponded to the rainy season, and the highest LST was seen in the dry season. The seasonal pattern is influenced by the southwest monsoon more than the northeast (Sa'adi et al., 2019).

There were five out of the eight super-regions had significant rises in day LST. Some studies in Malaysia showed a close result where temperature rises happened within reach the end of the year (Ismail et al., 2019). The same outcomes in four seasons area revealed that the highest LST emerged during the summer between June and September (Khorchani et al., 2018; Singh et al., 2014).

We detected the mean LST in Borneo Island raised by $0.203^{\circ}C$ per decade, or $2^{\circ}C$ per century, and was lower than the mean rise surface temperature of $3\text{-}5^{\circ}C$ per century predicted by Tangang et al. (2012). The variation in LST on Borneo Island was highly significant. The rise in change impacts deforestation and LU change (Wolff et al., 2018).

Variations in LST would be affected by the variety of LC, mostly vegetation. The regions with a low vegetation index could have high LST (Buyadi et al., 2014). Healthy vegetation would be a porous medium, thus inhibiting any rising surface temperatures. Green vegetation will engage sunlight radiation and employ it for photosynthesis (Babalola and Akinsanola, 2016). Deviations correspondingly predisposed temperature rises in Borneo in the vegetation of the island (Evans, 2020). Deforestation was accepted to be a cause for increasing temperatures in the landmass area. The low vegetation index in Borneo decorates the rise in LST temperatures (Suherman et al., 2014).

The temperature changes in an area were triggered by variations in LC processed, such as deforestation or reforestation (Prevedello et al., 2019). Earlier studies also introduced that LU/LC variation affects LST (Majumderet al., 2018; Odindi et al., 2015; Rasul et al., 2017). If the LC in an area decline, the temperature can rise (Parmesan and Hanley, 2015). Studies in Borneo have observed that interconnected variations in LC and LST show that both variables are correlated, affecting human prosperity (Wolff et al., 2018). Some Studies from Malaysia also expressed that the warmest temperatures are built-up areas, and the coldest zones are in forest and mangrove areas (Sheikhi and Devi, 2018). Other studies have also supported that land-use change has a substantive effect on climate variation (Scott et al., 2018).

The correlation coefficient average between LST and NDVI in Boneo Island was low and varied for each sub-region. Most of the correlation coefficient of the sub-region has a positive correlation value with a significant result. The result is different from the correlation between NDVI and surface temperature in Perak and Kedah States, Malaysia. The research has a negative correlation coefficient, the NDVI decreased, and LST increased. Both states have reduced NDVI from 0.6 to 0.5 over 29 years (Jaafar et al., 2020). Sun and Kafatos (2007) found in North America that a positive correlation between LST and NDVI in the winter season and a negative correlation in summer. The positive correlation is also influenced by the sea surface temperature impact on LST (Yan et al., 2020).

The LST and NDVI pattern showed two main patterns on Borneo Island. Most of the sub-regions depict an increase in the LST and NDVI curves from the beginning of the year and show curves that are apart in LST and NDVI in the middle of the year. There is slight increase in LST and NDVI at the end of the year. As for the rest of the

sub-regions, the LST and NDVI curves have increased from the beginning of the year. Flatted together LST and NDVI in the middle of the year. As for the end of the year, there is a slight increase in LST and NDVI. Change in NDVI pattern in Borneo Island does not follow the LST pattern because of other factors such as a forest fire (Bontemps and Defourny, 2007).

5.2 Conclusion

There was a seasonal pattern and sub-regions of New Guinea and Borneo Island. We have shown that the cubic spline model with seven knots gave a significant mean increase of LST per decade variation on New Guinea and Borneo Island. The result for the New Guinea Island shows that many parts of New Guinea Island have an LST increase. The 45 sub-regions distance has a not significant mean of LST variation compared to 90 sub-regions that have shown an increase in the variation of the LST on the New Guinea Island. The mean increase of LST for the 45 sub-regions is +0.012°C per decade with no significant confidence interval (-0.052, 0.077)°C, and the mean of LST for this research on 90 sub-region is +0.086°C per decade with a significant confidence interval (0.028, 0.144)°C. It also shows that the LST variation occurs at the sub-region level.

The cubic spline model was applied to examine the LST pattern and variation on Borneo Island. The study designated a statistically significant rise in the mean LST variation in Borneo for eight super-regions with an average increase of +0.203°C (0.138 – 0.267)°C. Significant rises in LST were for super-region Sarawak, West Kalimantan, East Kalimantan, West-central Kalimantan, and Central-east Kalimantan. Among the remaining three super-regions, the LST in super-region Sabah & Brunei slightly

declined, East Kalimantan slightly raised, and in South Kalimantan super-regions, the trend was steady.

5.3 Limitation and recommendation

This research was examined the LST and Normalized Difference Vegetation Index (NDVI) using the cubic spline model and linear model with the big islands such as New Guinea and Borneo Island on the equator line. The following research could use the cubic spline model with different numbers and knots placement to examine the seasonal pattern and the LST variation. The appropriate distance between sub-regions for the small island is also considered. We also need to explore this method to another big island along the equator or the poles to precisely verify the finding. The island of New Guinea and Borneo Island consists of many mountains and plants as a typical tropical area. This other factor that affects the LST, such as LE, LU/LC, and the type of vegetation that will affect the LST change, could be reviewed in the following study.

This study was used a 105-pixel distance between the sub-regions to have a representative sample point covering the island and avoid the spatial correlation with result narrow and significant confidence interval. The appropriate distance between sub-regions was also considered in the subsequent study for the small island.

LST increased in New Guinea, and Borneo Island is signalled regional climate change. Further studies are demanded to authenticate the results of this study on a broader scale. Other techniques are required to refine the precision and approximation, applying other large islands located in latitudes far from the equator, such as Greenland. In the analysis, the inclusion of different variables for instance NDVI, LE, and LC may also be essential because most large islands suppress mountains and LU change.

The Pearson correlation was used to examine the correlation between LST and NDVI on Borneo Island with the low correlation coefficient. It is possible for further research to add the new variable and different location and the size of the area on the earth related to LST variation uses other statistical methods besides the cubic spline to assess the LST change, trend, and correlation. Furthermore, investigating the relationship between LST and monsoon season and precipitation on New Guinea and Borneo Island.

References

Aburas, M. M., Abdullah, S. H., Ramli, M. F. and Ash'aari, Z. H. 2015. Measuring land cover change in Seremban, Malaysia using NDVI index. Procedia Environmental Sciences, 30, 238-243.

Aharon, P. and Chappell, J. 1986. Oxygen isotopes, sea level changes and the temperature history of a coral reef environment in New Guinea over the last 105 years. Palaeogeography, Palaeoclimatology, Palaeoecology, 56(3-4), 337-379.

Alavipanah, S., Wegmann, M., Qureshi, S., Weng, Q. and Koellner, T. 2015. The role of vegetation in mitigating urban land surface temperatures: a case study of Munich, Germany during the warm season. Sustainability, 7(4), 4689-4706.

Armstrong, B. 2006. Models for the relationship between ambient temperature and daily mortality. Epidemiology, 624-631.

Anton, H. and Rorres, C. 2010. Elementary linear algebra: applications version. John Wiley and Sons, New Jersey, U.S.A., pp. 546.

Ayuningtyas, V. A. 2015. Pengolahan data thermal (TIRS) citra satelit Landsat 8 untuk temperatur suhu permukaan (Studi lokasi : Kabupaten Banyuwangi) (pp. 1–8).

Babalola, O. and Akinsanola, A. 2016. Change detection in land surface temperature and land use land cover over Lagos Metropolis, Nigeria. Journal of Remote Sensing & GIS, 5(3), 2–7.

Batatia, H. and Bessaih, N. 1997. Satellite land surface temperature for Sarawak area. In Proceedings of the 1997 Asian Conference on Remote sensing. Global Environment Session.

Bontemps, S. and Defourny, P. 2007. Mapping forest change in Borneo in 2000-2006
by a multispectral statistically-based detection technique with SPOT-
VEGETATION. In 2007 International Workshop on the Analysis of Multi-
temporal Remote Sensing Images (pp. 1-6).

Bourke, R. M. 2010. Altitudinal limits of 230 economic crop species in Papua New
Guinea. Altered ecologies: fire, climate and human influence on terrestrial
landscapes. Canberra: The Australian National University, 473-512.

Buyadi, S. N. A., Mohd, W. M. N. W. and Misni, A. 2014. Impact of vegetation
growth on urban surface temperature distribution. IOP Conference Series: Earth
and Environmental Science, 18(1), 1–7.

Case, M., Ardiansyah, F. and Spector, E. 2007. Climate change in Indonesia:
implications for humans and nature. Available online:
http://wwf.panda.org/wwf_news/?118240/. [March 11, 2018]

Checkley, W., Epstein, L. D., Gilman, R. H., Figueroa, D., Cama, R. I., Patz, J. A. and
Black, R. E. 2000. Effects of EI Niño and ambient temperature on hospital
admissions for diarrhoeal diseases in Peruvian children. The
Lancet, 355(9202), 442-450.

Chooprateep, S. and McNeil, N. 2014. Temperature changes in Southeast Asia: 1973-
2008. Chiang Mai University Journal of Natural Science, 13, 105-116.

Cleary, M. C. and Lian, F. J. 1991. On the geography of Borneo. Progress in Human
Geography, 15(2), 163-177.

Collins, N. M., Sayer, J. and Whitmore, T. C. 1991. The conservation atlas of tropical
forests: Asia and the Pacifics. Macmillan Press Ltd, London and Basingstoke,
UK, pp. 207.

Cooke, F. M. 2006. State, communities and forests in contemporary Borneo (p. 208). ANU Press.

Cruz, J. 2007. Ocean wave energy: current status and future perspectives. Springer Science & Business Media.

Davies, J. M., Dunne, R. P. and Brown, B. E. 1997. Coral bleaching and elevated sea-water temperature in Milne Bay Province, Papua New Guinea, 1996. Marine and Freshwater Research, 48(6), 513-516.

Davis, A. J., Holloway, J. D., Huijbregts, H., Krikken, J., Kirk-Spriggs, A. H. and Sutton, S. L. 2001. Dung beetles as indicators of change in the forests of northern Borneo. Journal of Applied Ecology. 38(3), 593-616.

Dullinger, S., Dirnböck, T. and Grabherr, G. 2004. Modelling climate change-driven treeline shifts: relative effects of temperature increase, dispersal and invasibility. Journal of Ecology, 92(2), 241-252.

Dunstone, N. J. 2014. A perspective on sustained marine observations for climate modelling and prediction. Philosophical Transactions. Series A, Mathematical, Physical, and Engineering Sciences, 372(2025), 20130340. https://doi.org/10.1098/rsta.2013.0340

Estoque, R. C., Murayama, Y. and Myint, S. W. 2017. Effects of landscape composition and pattern on land surface temperature: An urban heat island study in the megacities of Southeast Asia. Science of the Total Environment. 577, 349-359.

Evans, M. 2020. Forest loss leads to local climate change effect in Borneo. Retrieved from Landscape News website:

https://news.globallandscapesforum.org/27161/forest-loss-leads-to-local-climate-change-effect-in-borneo/

Feng, Y., Gao, C., Tong, X., Chen, S., Lei, Z. and Wang, J. 2019. Spatial patterns of land surface temperature and their influencing factors: a case study in Suzhou, China. Remote Sensing. 11(2), 182.

Foley, J. A., Defries, R., Asner, G. P., Barford, C., Bonan, G., Carpenter, S. R., Chapin, F. S., Coe, M. T., Daily. G.C., Gibbs, H. K., Helkowski, J. H., Holloway, T., Howard, E. A., Kucharik, C. J., Monfreda, C., Patz, J. A., Prentice, I. C., Ramankutty, N. and Snyder, P. K. 2005. Global consequences of land use. science, 309(5734), 570-574.

Folland, C. K., Salinger, M. J., Jiang, N. and Rayner, N. A. 2003. Trends and variations in South Pacific Island and ocean surface temperatures. Journal of Climate, 16(17), 2859–2874.

Fu, P. and Weng, Q. 2016. A time series analysis of urbanization induced land use and land cover change and its impact on land surface temperature with Landsat imagery. Remote Sensing of Environment, 175, 205–214.

Gao Y, Chen F, Barlage M, Liu W, Cheng G, Li X, Yu Y, Ran Y, Li H, Peng H. and Ma, M. 2008. Enhancement of land surface information and its impact on atmospheric modeling in the Heihe River Basin, northwest China. Journal of Geophysical Research: Atmospheres, 113(D20).

Gülüm, M., Yesilyurt, M. K. and Bilgin, A. 2019. The performance assessment of cubic spline interpolation and response surface methodology in the mathematical modeling to optimize biodiesel production from waste cooking oil. Fuel, 255, 115778.

Hashim, H., Abd Latif, Z. and Adnan, N. A. 2019. Urban vegetation classification with NDVI threshold value method with very high resolution (VHR) PLEIADES Imagery. Int. Arch. Photogramm. Remote Sens. Spat. Inf. Sci, 237-240.

Heritage, B. 2020. About Borneo. Retrieved from The Borneo Project website: https://borneoproject.org/borneo-2

Hidayati, I. C., Nalaratih, N., Shabrina, A., Wahyuni, I. N. and Latifah, A. L. 2020. Correlation of climate variability and burned area in Borneo using clustering methods. Forest and Society, 280-293.

How Jin Aik, D., Ismail, M. H., Muharam, F. M. and Alias, M. A. 2021. Evaluating the impacts of land use/land cover changes across topography against land surface temperature in Cameron Highlands. Plos One, 16(5), e0252111.

Houghton, J.T., Ding, Y.D.J.G., Griggs, D.J., Noguer, M., van der Linden, P.J., Dai, X. and Johnson, C.A. 2001. Climate change 2001: the scientific basis. The Press Syndicate of the University of Cambridge. 1035-1040.

Hughes, A. C. 2017. Understanding the drivers of Southeast Asian biodiversity loss. Ecosphere, 8(1). https://doi.org/10.1002/ecs2.1624

Hyndman, R. J. and Athanasopoulos, G. 2018. Forecasting: principles and practice. OTexts.

International Climate Change Adaptation Initiative. 2007. Current and future climate of Papua New Guinea. In Pacific climate change science program. Retrieved January 1, 2020, from http://www.pacificclimatechangescience.org/wp-content/uploads/2013/06/14_PCCSP_PNG_8pp.pdf

Ismail, N. A., Zawiah, W., Zin, W., Ibrahim, W. and Yeun, L. C. 2019. Eight-day daytime land surface temperature pattern over peninsular Malaysia. International Journal of Recent Technology and Engineering, 8(4), 11949–11955.

Jackson, R. T. and Standish, William. 2019. Papua New Guinea. Encyclopedia britannica. https://www.britannica.com/place/Papua-New-Guinea

Karl, T. R. and Trenberth, K. E. 2003. Modern global climate change. Science, 302(5651), 1719-1723.

Karnieli, A., Agam, N., Pinker, R. T., Anderson, M., Imhoff, M. L., Gutman, G. G., Panov, N. and Goldberg, A. 2010. Use of NDVI and land surface temperature for drought assessment: merits and limitations. Journal of Climate, 23(3), 618-633.

Kemarau, R. A. and Eboy, O. V. 2020. Urbanization and it impacts to land surface temperature on small medium size city for year 1991, 2011 and 2018: case study Kota Kinabalu. Journal of Borneo Social Transformation Studies, 6(1), 58-76.

Kestens, Y., Brand, A., Fournier, M., Goudreau, S., Kosatsky, T., Maloley, M. and Smargiassi, A. 2011. Modelling the variation of land surface temperature as determinant of risk of heat-related health events. International Journal of Health Geographics, 10(1), 7.

Khandelwal, S., Goyal, R., Kaul, N. and Mathew, A. 2018. Assessment of land surface temperature variation due to change in elevation of area surrounding Jaipur, India. The Egyptian Journal of Remote Sensing and Space Science. 21(1), 87-94.

Khorchani, M., Martin-Hernandez, N., Sergio, M., Vicente-Serrano, Azorin-Molina, C., Garcia, M., Domínguez-Duran, M. a. A., Reig, F., Pena-Galardo, M. and

Domínguez-Castro, F. 2018. Average annual and seasonal land surface temperature, spanish peninsular. Journal of Maps, 14(2), 465–475.

Kottawa-Arachchi, J. D. and Wijeratne, M. A. 2017. Climate change impacts on biodiversity and ecosystems in Sri Lanka: a review. Nature Conservation Research, 2(3), 2–22.

Korada, N., Sekac, T., Jana, S. K. and Pal, D. K. 2018. Delineating drought risk areas using remote sensing and geographic information systems – a case study of western highlands province, Papua New Guinea. European Journal of Engineering Research and Science, 3(10), 103–110.

Langner, A., Miettinen, J. and Siegert, F. 2007. Land cover change 2002–2005 in Borneo and the role of fire derived from MODIS imagery. Global Change Biology. 13(11), 2329-2340.

Li, Y., Zhang, H. and Kainz, W. 2012. Monitoring patterns of urban heat islands of the fast-growing Shanghai metropolis, China: using time-series of Landsat TM/ETM+ data. International Journal of Applied Earth Observation and Geoinformation, 19, 127–138.

Majumder, A., Kingra, P. K., Setia, R., Singh, S. P. and Pateriya, B. 2018. Influence of land use/land cover changes on surface temperature and its effect on crop yield in different agro-climatic regions of Indian Punjab. Geocarto International, 1–24.

Malcher, J. and Schönwiese, C. D. 1987. Homogeneity, spatial correlation and spectral variance analysis of long European and North American air temperature records. Theoretical and Applied Climatology, 38(3), 157-166.

Mardia, K. V., Kent, J. T and Bibby, J. M. 1979. Multivariate analysis (10th ed.; Z. W. Birbaum and E. Likacs, Eds.). San Diego: Academic Press, Inc.

Marjuki, Van Der Schrier, G., Tank, A. M. K., Van Den Besselaar, E. J. and Swarinoto, Y. S. 2016. Observed trends and variability in climate indices relevant for crop yields in Southeast Asia. Journal of Climate, 29(7), 2651-2669.

Mboera, L. E., Mayala, B. K., Kweka, E. J. and Mazigo, H. D. 2011. Impact of climate change on human health and health systems in Tanzania: a review. Tanzania journal of health research, 13(5).

McAlpine, C.A., Johnson, A., Salazar, A., Syktus, J., Wilson, K., Meijaard, E. and Sheil, D. 2018. Forest loss and Borneo's climate. Environmental Research Letters. 13(4), 1-11.

McNeil, N. and Chirtkiatsakul, B. 2016. Statistical models for the pattern of sea surface temperature in the North Atlantic during 1973-2008. International Journal of Climatology. 36:3856-3863.

Measey, M. 2010. Indonesia: a vulnerable country in the face of climate change. Global Majority E-Journal, 1(1), 31-45.

Mildrexler, D. J., Zhao, M., Cohen, W. B., Running, S. W., Song, X. P. and Jones, M. O. 2018. Thermal anomalies detect critical global land surface changes. Journal of Applied Meteorology and Climatology, 57(2), 391-411.

Mishra, A. K., Singh, V. P. and Jain, S. K. 2010. Impact of global warming and climate change on social development. Journal of Comparative Social Welfare, 26(2-3), 239-260.

Modland tile calculator. 2018. Available from:

> https://landweb.modaps.eosdis.nasa.gov/cgi-bin/developer/tilemap.cgi.

> Accessed in September 2018.

Mokarram, M. and Sathyamoorthy, D. 2015. Modeling the relationship between

> elevation, aspect and spatial distribution of vegetation in the Darab Mountain,

> Iran using remote sensing data. Modeling Earth Systems and

> Environment, 1(4), 1-6.

Munawar, Prasetya, T.A., McNeil, R. and Jani, R. 2020. Pattern and trend of land

> surface temperature change on New Guinea Island. Pertanika Journal of

> Science and Technology, 28. https://doi.org/10.47836/pjst.28.4.20

Munawar, M., Prasetya, T.A.E., McNeil, R. and Jani, R. 2022. Statistical modeling

> for land surface temperature in Borneo island from 2000 to 2019. Theoretical

> and Applied Climatology. https://doi.org/10.1007/s00704-021-03891-8

Odindi, J. O., Bangamwabo, V. and Mutanga, O. 2015. Assessing the value of urban

> green spaces in mitigating multi-seasonal urban heat using MODIS land surface

> temperature (LST) and Landsat 8 data. International Journal of Environmental

> Research, 9(1), 9–18.

ORNL DAAC. 2018. MODIS and VIIRS land products global subsetting and

> visualization tool. https://doi.org/10.3334/ornldaac/1379. Accessed in

> September 2018.

Parmesan, C. and Hanley, M. E. 2015. Plants and climate change: complexities and

> surprises. Annals of Botany, 116(6), 849–864.

Pascual, M., Bouma, M. J. and Dobson, A. P. 2002. Cholera and climate: revisiting

> the quantitative evidence. Microbes and Infection, 4(2), 237-245.

Prevedello, J. A., Winck, G. R., Weber, M. M., Nichols, E. and Sinervo, B. 2019. Impacts of forestation and deforestation on local temperature across the globe. Plos One, 14(3), 1–18.

Team, R. C. 2017. R: A language and environment for statistical computing [Internet]. Vienna, Austria; 2018. https://www.r-project.org/ (accessed Feb. 02, 2019).

Turner, B. L., Skole, D., Sanderson, S., Fischer, G., Fresco, L. and Leemans, R. 1995. Land-use and land-cover change: science/research plan.

Rasul, A., Balzter, H., Smith, C., Remedios, J., Adamu, B., Sobrino, J., Srivanit, M. and Weng, Q. 2017. A review on remote sensing of urban heat and cool islands. Land, 6(2), 38.

Rencher, A. C. and Schaalje, G. B. 2008. Linear models in Statistics. John Wiley and Sons, New Jersey, U.S.A., pp. 2.

Robiansyah, I. 2018. Assessing the impact of climate change on the distribution of endemic subalpine and alpine plants of New Guinea. Songklanakarin Journal of Science and Technology, 40(3), 701–709.

Sa'adi, Z., Shahid, S., Ismail, T., Chung, E. S. and Wang, X. J. 2019. Trends analysis of rainfall and rainfall extremes in Sarawak, Malaysia using modified Mann–Kendall test. Meteorology and Atmospheric Physics, 131(3), 263-277.

Sahoo, N. and Peetala, R. K. 2010. Transient temperature data analysis for a supersonic flight test. Journal of heat transfer, 132(8).

Samanta, S. 2009. Assessment of surface temperature using remote sensing technology. Papua New Guinea Journal of Research, Science and Technology, 1, 12-18.

Scott, C. E., Monks, S. A., Spracklen, D. V, Arnold, S. R., Forster, P. M., Rap, A., Aijala, M., Artaxo, P., Karslaw, K. S., Chipperfield, M. P., Ehn, S.,Gilardoni, S., Heikkinen, L., Kulmala, M., Petäjä, T., Reddington, C. L. S., Rizzo, L. V., Swietlicki, E., Vignati, E. and Wilson, C. 2018. Impact on short-lived climate forcers increases projected warming due to deforestation. Nature Communications, 9(157), 1–9.

Sheikhi, A. and Devi, K. 2018. Impact of land cover change on urban surface temperature in Iskandar Malaysia. Chemical Engineering Transactions, 63(Im), 25–30.

Singh, R. B., Grover, A. and Zhan, J. 2014. Inter-seasonal variations of surface temperature in the urbanized environment of Delhi using Landsat thermal data. Energies, 7(3), 1811–1828.

Suherman, A., Rahman, M. Z. A. and Busu, I. 2014. Albedo and land surface temperature shift in hydrocarbon seepage potential area, case study in Miri Sarawak Malaysia Albedo and land surface temperature shift in hydrocarbon seepage potential area, case study in Miri Sarawak Malaysia. 8th International Symposium of the Digital Earth (ISDE8), 012148. https://doi.org/10.1088/1755-1315/18/1/012148

Sun, D. and Kafatos, M. 2007. Note on the NDVI-LST relationship and the use of temperature-related drought indices over North America. Geophysical Research Letters, 34(24).

Sun, Q., Wu, Z. and Tan, J. 2012. The relationship between land surface temperature and land use/land cover in Guangzhou, China. Environmental Earth Sciences, 65(6), 1687-1694.

Storch, H. V. 1999. Misuses of statistical analysis in climate. In von Storch H., Navarra A. (eds) Analysis of climate variability. Springer Berlin Heidelberg. https://doi.org/10.1007/978-3-662-03744-7

Storch, H. V. and Zwiers, F. W. 1999. The statistical description and understanding of climate. Statistical Analysis in Climate Research. https://doi.org/10.1017/CBO9780511612336

Tangang, F. T., Juneng, L., Salimun, E., Sei, K. M., Le, L. J. and Muhamad, H. 2012. Climate change and variability over Malaysia: gaps in science and research information. Sains Malaysiana, 41(11), 1355–1366.

Jaafar, W. S. W. M, Maulud, K. N. A, Kamarulzaman, A. M. M, Raihan, A., Sah, S. M, Ahmad, Saad, S. N. M. A, Azmi, A. T. M., Syukri N. K. A. J. and Khan, W. R. 2020. The influence of deforestation on land surface temperature - a case study of Perak and Kedah, Malaysia. Forests, 11(6), 670.

Wan, Z., Zhang, Y., Zhang, Q. and Li, Z.L. 2004. Quality assessment and validation of the MODIS global land surface temperature. International Journal of Remote Sensing. 25(1), 261-274.

Wang, H., Yang, Z., Saito, Y., Liu, J. P., Sun, X. and Wang, Y. 2007. Stepwise decreases of the Huanghe (Yellow River) sediment load (1950–2005): impacts of climate change and human activities. Global and Planetary Change, 57(3-4), 331-354.

Wang, M., Jiang, A., Gong, L., Luo, L., Guo, W., Li, C., Yang, B, Zeng, J., Chen, Y., Zheng, K. and Li, H. 2020. Temperature significant change COVID-19 transmission in 429 cities. medrxiv.

Weigand, M., Wurm, M., Dech, S. and Taubenböck, H. 2019. Remote sensing in environmental justice research-a review. ISPRS International Journal of Geo-Information, 8(1).

Wheeler, T. and Von Braun, J. 2013. Climate change impacts on global food security. Science, 341(6145), 508-513.

Wolff, N. H., Masuda, Y. J., Meijaard, E., Wells, J. A. and Game, E. T. 2018. Impacts of tropical deforestation on local temperature and human well-being perceptions. Global Environmental Change, 52(July), 181–189.

Wongsai, N., Wongsai, S. and Huete, A. 2017. Annual seasonality extraction using the cubic spline function and decadal trend in temporal daytime MODIS LST data. Remote Sensing, 9(12), 1254.

Wu, X., Lu, Y., Zhou, S., Chen, L. and Xu, B. 2016. Impact of climate change on human infectious diseases: empirical evidence and human adaptation. Environment international, 86, 14-23.

Yan, Y., Mao, K., Shi, J., Piao, S., Shen, X., Dozier, J., Liu, Y Ren, H. and Bao, Q. 2020. Driving forces of land surface temperature anomalous changes in North America in 2002–2018. Scientific reports, 10(1), 1-13.

Yue, W., Xu, J., Tan, W. and Xu, L. 2007. The relationship between land surface temperature and NDVI with remote sensing: application to Shanghai Landsat 7 ETM+ data. International journal of remote sensing, 28(15), 3205-3226.

Appendix

Appendix 1 Article "Pattern and Trend of Land Surface Temperature on New Guinea Island"

Pattern and Trend of Land Surface Temperature Change on New Guinea Island

Munawar[1,2], Tofan Agung Eka Prasetya[1,3], Rhysa McNeil[1,4]* and Rohana Jani[5]

[1]*Faculty of Science and Technology, Prince of Songkla University, Pattani Campus, Muang Pattani, 94000 Thailand*
[2]*Faculty of Mathematics and Science, Syiah Kuala University, Jl. Syech Abd.Rauf, Kopelma Darussalam, Banda Aceh, Aceh 23111, Indonesia*
[3]*Vocational Faculty, Universitas Airlangga, Jl. Dharmawangsa Dalam Selatan No 68, Airlangga, Gubeng, Surabaya, East Java, Indonesia*
[4]*Centre of Excellence in Mathematics, Commission on Higher Education (CHE), Ministry of Education, Ratchathewi, Bangkok, 10400 Thailand*
[5]*Faculty of Economics and Administration, University of Malaya, 50603 UM, Kuala Lumpur, Malaysia*

ABSTRACT

Global warming will have an impact on nature in many ways, including rising sea levels and an increasing spread of infectious diseases. Land surface temperature is one of the many indicators that can be used to measure climate change on both a local and global scale. This study aims to analyze the change in land surface temperatures on New Guinea Island using a cubic spline method, autoregressive model, and multivariate regression. New Guinea Island was divided into 5 regions each consisting of 9 subregions. The data of each subregion was obtained from the National Aeronautics and Space Administration moderate resolution imaging spectroradiometer database from 2000 to 2019. The average change in temperature was +0.012°C per decade. However, the changes differed by region; significantly decreasing in the northwest at -0.107°C per decade (95% CI: -0.207, -0.007), significantly increasing in the south at 0.201°C per decade (95% CI: 0.069, 0.333), and remaining stable in the centralnorth, southeast and northeast.

Keywords: Cubic spline, global warming, land surface temperature, New Guinea Island

Appendix 2 Proceeding "Sumatra Land Surface Temperature Increase"

Sumatra Land Surface Temperature Increase

M Munawar[1,2,*] T A E Prasetya[1,3] R McNeil[1,4] R Jani[5]

[1] *Research Methodology Department, Faculty of Science and Technology, Prince of Songkla University, Pattani Campus, Muang Pattani, 94000 Thailand*

[2] *Statistics Department, Faculty of Mathematics and Science, Syiah Kuala University, Jl. Syech Abd.Rauf, Kopelma Darussalam, Banda Aceh, Aceh 23111, Indonesia*

[3] *Health department, Faculty of Vocational Studies, Universitas Airlangga, Indonesia*

[4] *Centre of Excellence in Mathematics, Commission on Higher Education (CHE), Ministry of Education, Ratchathewi, Bangkok, 10400 Thailand*

[5] *Ungku Aziz Centre for Development Studies, Faculty of Economics & Administration, University Malaya, Malaysia*

[*]*Corresponding author. Email:* munawar@unsyiah.ac.id

ABSTRACT

Climate change in Sumatra island is likely a result of widespread land-use changes by the plantation industry. This study aims to investigate trends in land surface temperatures in Sumatra island. Land surface temperatures from 2001-2020 were downloaded from the National Aeronautics and Space Administration moderate resolution imaging spectroradiometer Terra satellite and divided into 5 regions and 45 sub-regions spread equally across the island. The statistical method that used to analyzed the data was cubic spline and multiple regression. The seasonal pattern and variation in the land surface temperature were examined using a cubic spline method and the seasonally adjusted land surface temperature was analyzed using a multiple regression model. On average, the land surface temperature on Sumatra island significantly increased over the ten years by $0.076°C$ with a 95% confidence interval of [0.010, 0.141]°C.

Keywords: Climate change, Land surface temperature, Cubic spline, Sumatra island.

1. INTRODUCTION

Global warming and climate change are global problems that are currently being discussed with various disciplines trying to find solutions [1]. The temperature increase is an important indicator of climate change. It can cause a rise in sea levels, escalate the spread of disease, and result in food deficiency due to crop failure [2], [3].

A study shows that the world will experience a temperature increase probable to reach 1.5°C between 2030 and 2052 [4]. Temperatures in the Southeast Asia region are predicted to continue to increase with average temperatures increasing every decade since 1960 [5]. In Indonesia, the temperature is projected to become warmer by $0.2 – 0.3°C$ per decade, and Sumatra and Borneo islands will change in the season[6]. Sumatra island relies on agriculture and fishery products as its main source of income. Climate change in Sumatra island is believed to be caused by land-use change by the plantation industry [7]. Therefore, this research will examine the seasonal pattern and the increased variation of Land Surface Temperature (LST) in Sumatra island.

2. METHODS

Sumatra island is divided into 5 regions with each consisting of 9 equally spread subregions 95 km apart to avoid overlap and spatial correlation. LST was downloaded from the National Aeronautics and Space Administration moderate resolution imaging spectroradiometer (NASA MODIS) Terra satellite from 2001 to 2020 [8].

The seasonal pattern of LST was examined through the combination of a cubic spline model and a linear regression model as shown below [9]:

$$a + bt + \sum_{k}^{p-3} c_k \left[(t - t_k)_+^3 - d(t - t_{p-2})_+^3 + e(t - t_{p-1})_+^3 - f(t - t_p)_+^3 \right]$$

(1)

Appendix 3 Article "Statistical modelling for land surface temperature in Borneo island from 2000 to 2019"

ORIGINAL PAPER

Statistical modeling for land surface temperature in Borneo island from 2000 to 2019

Munawar Munawar[1,2] · Tofan Agung Eka Prasetya[1,3] · Rhysa McNeil[1,4] · Rohana Jani[5]

Abstract

Increased temperature is one of the signals of global warming. Trends in land surface temperature can be used to measure climate change. This research aimed to investigate the variation of land surface temperature in Borneo island using a cubic spline method and a multivariate regression model. The island was divided into 8 regions each comprising 9 subregions. Land surface temperatures for each subregion from 2000 to 2019 were obtained from the National Aeronautics and Space Administration Moderate Resolution Imaging Spectroradiometer database. The average increase in temperature was 0.2 °C/decade with a 95% confidence interval of (0.14, 0.27) °C. The changes differed by region; a significant increase was seen in Sarawak, North Kalimantan, West Kalimantan, West-central Kalimantan, and Central-east Kalimantan region; a slight decrease in Sabah and Brunei Darussalam (Sabah and Brunei) region; a slight increase in East Kalimantan; and a stable trend in South Kalimantan.

1 Introduction

The world is currently facing many environmental issues including global warming. Rising temperatures are one of the signals of global warming. Land surface temperatures (LST) can provide an overview of climate change on a regional and global scale (Zhang and Liang 2018). Climate change can result in damage to human society and the environment (Trenberth 2018) and is predicted to influence public health due to heatwaves, vector-borne diseases such as malaria, respiratory illness (Coleman and Frieman 2014), food resource deficiency, and other human health problems (Bell and Greenberg 2018). In the long term, these problems will have an impact on social and economic aspects globally (Tol 2018).

Many countries around the world are starting to pay attention to the climate change. An increase in LST in an area becomes an important indicator to determine certain policies related to climate change (Fox et al. 2019). Shanghai City is the biggest city in China with massive development with large changes in land use or land cover. This situation has changed the land surface characteristic and spatiotemporal pattern of urban heat island which is designated by LST (Li et al. 2012). Some parts of Southeast Asia such as Kalimantan in Indonesia, East Malaysia, and Brunei Darussalam have experienced land use changes, mainly for oil palm cultivation (Gunarso et al. 2013). Countries in Southeast Asia are facing LST issues as a result of development policies. The average LST increases in Malaysia during 1990–2015 were between 25.4 and 32.7 °C and in Indonesia during 1989–2018 were between 26.6 and 27.6 °C (Hua and Ping 2018; Himayah et al. 2019). In other Southeast Asian countries, such as Thailand, the mean daily maximum temperature is predicted to increase by 1.2 to 1.9 °C by 2050 (Marks 2011).

Kalimantan island is the third largest island after Greenland and New Guinea (Heritage 2020). Most of the islands belong to Indonesia, and the remaining islands belong to Malaysia and Brunei Darussalam. Kalimantan has lowlands,

✉ Rhysa McNeil
  rhysa.m@psu.ac.th

[1] Faculty of Science and Technology, Prince of Songkla University, Pattani Campus, Muang, Pattani 94000, Thailand

[2] Faculty of Mathematics and Science, Syiah Kuala University, Jl. Syech Abd.Rauf, Kopelma Darussalam, Banda Aceh, Aceh 23111, Indonesia

[3] Health Department, Faculty of Vocational Studies, Universitas Airlangga, Surabaya, Indonesia

[4] Centre of Excellence in Mathematics, CHE, Si Ayutthaya Rd., Bangkok 10400, Thailand

[5] Ungku Aziz Centre for Development Studies, Faculty of Economics & Administration, University Malaya, Kuala Lumpur, Malaysia

🦋 Springer

VITAE

Name   Mr. Munawar

Student ID   6120330010

Educational Attainment

Degree	Name of Institution	Year of Graduation
Master of Applied Statistics	Universiti Malaya	2008
Bachelor of Mathematics	Syiah Kula University	1999

Scholarship Awards during Enrolment

- Thailand's Education Hub for ASEAN Countries (TEH AC)

- Graduate School of Prince of Songkla University Research Grant, Thailand

- The Centre of Excellence in Mathematics, Commission on Higher Education, Thailand.

Work – Position and Address

- Senior lecturer in Department of Statistics, Faculty of Mathematics and Science, Syiah Kuala University, Banda Aceh, Indonesia (2010 – now).

List of Publication and Proceeding

- Munawar, Prasetya, T.A., McNeil, R. and Jani, R. 2020. Pattern and Trend of Land Surface Temperature Change on New Guinea Island. Pertanika Journal of Science and Technology, 28. https://doi.org/10.47836/pjst.28.4.20

- Munawar, M., Prasetya, T. A. E., McNeil, R. and Jani, R. 2021. Sumatra Land Surface Temperature Increase. 1st International Conference on Mathematics and Mathematics Education (ICMMEd 2020) (pp. 89-92). Atlantis Press

- Munawar, M., Prasetya, T.A.E., McNeil, R. and Jani, R. 2022. Statistical modeling for land surface temperature in Borneo island from 2000 to 2019. Theoretical and Applied Climatology. https://doi.org/10.1007/s00704-021-03891-8

- Prasetya, T. A. E., Munawar, M., Taufik, M. R., Chesoh, S., Lim, A., and McNeil, D. 2020. Land Surface Temperature Assessment in Central Sumatra, Indonesia. Indonesian Journal of Geography, 52(2), 227-238

- Prasetya, T. A. E., Munawar, Chesoh, S., Lim, A. and McNeil, D. R. 2020. Different Space Characteristics of Air Temperature Variation in North Sumatra Indonesia. In Journal of Physics: Conference Series (Vol. 1517, No. 1, p. 012008). IOP Publishing

- Prasetya, E., Agung, T., Munawar, Chesoh, S., Lim, A. and McNeil, D. 2020. Systematic Measurement of Temperature Change in Sumatra Island: 2000-2019 MODIS Data Study. Journal of Climate Change, 6(1), 1-6.